

CAPITAL UNIVERSITY OF SCIENCE AND
TECHNOLOGY, ISLAMABAD



Screening of Active Constituents
of *Artemisia annua* Against Viral
Main Protease M^{pro}/CLpro of
SARS-CoV-2—an *Insilico* Study

by

Eraj Irfan

A thesis submitted in partial fulfillment for the
degree of Master of Science

in the

Faculty of Health and Life Sciences

Department of Bioinformatics and Biosciences

2021

Copyright © 2021 by Eraj Irfan

All rights reserved. No part of this thesis may be reproduced, distributed, or transmitted in any form or by any means, including photocopying, recording, or other electronic or mechanical methods, by any information storage and retrieval system without the prior written permission of the author.

I dedicate this thesis to my loving and supportive family and friends who have fully helped me in achieving my life goals.



CERTIFICATE OF APPROVAL

Screening of Active Constituents of *Artemisia annua*
Against Viral Main Protease M^{pro}/CLpro of
SARS-CoV-2—an *Insilico* Study

by

Eraj Irfan

(MBS193016)

THESIS EXAMINING COMMITTEE

S. No.	Examiner	Name	Organization
(a)	External Examiner	Dr. Aman Karim	NUMS, Rawalpindi
(b)	Internal Examiner	Dr. Sahar Fazal	CUST, Islamabad
(c)	Supervisor	Dr. Erum Dilshad	CUST, Islamabad

Dr. Erum Dilshad

Thesis Supervisor

December, 2021

Dr. Sahar Fazal

Head

Dept of Bioinformatics and Biosciences

December, 2021

Dr. M. Abdul Qadir

Dean

Faculty of Health and Life Sciences

December, 2021

Author's Declaration

I, **Eraj Irfan** hereby state that my MS thesis titled “**Screening of Active Constituents of *Artemisia annua* Against Viral Main Protease M^{pro}/CLpro of SARS-CoV-2—an *Insilico* Study.**” is my work and has not been previously submitted by me for taking any degree from Capital University or any other institute in-country or abroad.

If my statement is found incorrect by any means the university holds the right to cancel my MS degree at any time.

(Eraj Irfan)

Registration No: MBS193016

Plagiarism Undertaking

I, solemnly declare that research work presented under the title “**Screening of Active Constituents of *Artemisia annua* Against Viral Main Protease M^{pro}/CL^{pro} of SARS-CoV-2—an *Insilico* Study.**” is solely my research work with no significant contribution from any other person. Little help taken from any person has been acknowledged and that complete thesis has been written by me.

I surely understand the zero-tolerance policy of HEC and Capital University of Science and Technology, Islamabad towards plagiarism, for that I declare that no part of the thesis titled as mentioned above has been plagiarized and any material taken from any source has been referred properly.

I undertake that if the university finds me guilty for breaking the plagiarism rule then the university holds full right to withdraw my MS degree.

(Eraj Irfan)

Registration No: MBS193016

Acknowledgement

All praise and thanks to the Supreme God to whom we only bow down. I would also like to express my gratitude to my family and friends for their continuous mental and physical support and prayers. I would also wholeheartedly say a big thank you to my supervisor Dr. Erum Dilshad (Assistant Professor, Department of Bioinformatics and Biosciences, CUST) for her support with that I would say a special thanks to Dr. Naeem Mahmood Ashraf (Lecturer Biochemistry and Biotechnology, University of Gujrat) for giving his precious time to assist with computational study.

Thanks to all.

(Eraj Irfan)

Abstract

In November 2019, the whole world went into a major threatening situation with the announcement of the pandemic called SARS-CoV-19 or Covid-19. To control the spread of the disease many drugs were repurposed and certain instructions like that of use of sanitizers, social distancing, and application of face mask were made certain. With this, the whole scientific world was working to find a solution to stop this pandemic. For this purpose, many plants were exploited to find natural compounds to work against this virus. The detailed study of the SARS-CoV-19 shows that the non-structural protein M^{pro} is responsible for the cleavage of replicating enzymes. The active compounds in *Artemisia annua* were studied that could inhibit the protein M^{pro} . 25 ligands were selected for this purpose. The protein and the ligands were then docked against each other by CB dock. The interactions were visualized through pyMol and analyzed by LigPlot. These ligands were then screened out on the basis of Lipinski Rule and through studying the ADMET properties of the ligands. After the overall screening phase, the lead compound chrysopenetin was selected against the standard drug azithromycin. The comparative result shows that chrysopenetin can be more effective drug candidate against M^{pro} rather than azithromycin. However further research has to be carried out to investigate the plant's effectiveness against SARS-CoV-2.

Keywords: Covid-19, *Artemisia annua*, CB-dock, ADMET, Chrysopenetin, and Azithromycin.

Contents

Author's Declaration	iv
Plagiarism Undertaking	v
Acknowledgement	vi
Abstract	vii
List of Figures	xi
List of Tables	xiii
Abbreviations	xiv
1 Introduction	1
1.1 Problem Statement	3
1.2 Aim and Objectives of Study	3
2 Literature Review	4
2.1 SARS COV-2	4
2.2 Origin	5
2.3 Entry and Life Cycle	6
2.4 Symptoms	7
2.5 Treatment for Corona Virus	8
2.6 Medicinal Plants	9
2.7 <i>Artemisia annua</i>	10
2.8 Taxonomic Hierarchy	11
2.9 Active Constituents of <i>Artemisia annua</i>	12
2.10 Molecular Docking	13
2.11 3CL Protease	14
2.12 Natural Compounds as Inhibitors of 3CL Protease	15
2.13 Bioactive constituents of <i>Artemisia annua</i>	16
3 Materials And Methods	17
3.1 Selection of Protein	17

3.2	Determination of physicochemical Properties of Proteins	17
3.3	Cleaning of the Downloaded Protein	18
3.4	Determination of Functional Domains of Target Proteins	18
3.5	Selection of Active Metabolic Ligands	18
3.6	Ligand Preparation	18
3.7	Molecular Docking	19
3.8	Visualization of Docking Result via PyMol	19
3.9	Analysis of Docked Complex via LigPlot	20
3.10	Ligand ADME Properties	20
3.11	Lead Compound Identification	20
3.12	Comparison with the Standard Drug	21
4	Results and Discussion	22
4.1	Structure Modelling	22
4.1.1	3D Structure of the Protein	22
4.1.2	Physicochemical Properties of Protein	23
4.1.3	Identification of Functional Domains of the Protein	24
4.1.4	Structure of Protein Refined for Docking	25
4.2	Ligand Selection	25
4.3	Virtual Screening and Toxicity Prediction through Lipinski Rule of Five	28
4.3.1	Toxicity Prediction	30
4.4	Molecular Docking	33
4.5	Interaction of Ligands and Targeted Protein	36
4.6	ADME Properties of Ligand	59
4.6.1	Pharmacodynamics	59
4.6.2	Pharmacokinetics	59
4.6.3	Absorption	59
4.6.4	Distribution	62
4.6.5	Metabolism	65
4.6.6	Excretion	67
4.7	Lead Compound Identification	69
4.8	Drug Identification against Covid-19	70
4.8.1	Azithromycin	70
4.8.2	Azithromycin Docking	70
4.9	Azithromycin Comparison with Lead Compound	71
4.10	ADMET Properties Comparison	72
4.10.1	Toxicity Comparison	72
4.10.2	Absorption Properties Comparison	73
4.10.3	Metabolic Properties Comparison	74
4.10.4	Distribution Properties Comparison	74
4.10.5	Excretion Properties Comparison	75
4.11	Physicochemical Properties Comparison	76
4.12	Docking Score Comparison	77
4.13	Docking Analysis Comparison	77

5	Conclusion and Future Prospects	80
5.1	Recommendations	81
6	Bibliography	82

List of Figures

2.1	Structure of SARS-CoV-2 [13].	4
2.2	Sequence alignment of 22 Corona Viruses [15].	5
2.3	Entry and life cycle of the SARS-CoV-2 in the human cell [19].	7
2.4	<i>Artemisia annua</i> [35].	11
3.1	Methodology opted for this study.	21
4.1	6LU7 complexed with N3 inhibitor-the red dots show the inhibitor.	23
4.2	Functional domains of targeted protein.	24
4.3	6LU7 cleaned protein	25
4.4	Interaction of α -pinene with the receptor protein	37
4.5	Interaction of β -pinene with receptor protein	37
4.6	Interaction of carvone with receptor protein	38
4.7	Interaction of myrtenol with receptor protein	38
4.8	Interaction of quinic acid with receptor protein	39
4.9	Interaction of caffeic acid with receptor protein	39
4.10	Interaction of quercetin with receptor protein	40
4.11	Interaction of rutin with receptor protein	40
4.12	Interaction of apigenin with receptor protein	41
4.13	Interaction of chrysoplenetin with receptor protein	41
4.14	Interaction of arteannunin b with receptor protein	42
4.15	Interaction of artemisinin with receptor protein	42
4.16	Interaction of scopoletin at 3rd cavity with receptor protein	43
4.17	Interaction of scopoletin at 5th cavity with receptor protein	43
4.18	Interaction of scoparone with receptor protein	44
4.19	Interaction of artemisnic acid with receptor protein	44
4.20	Interaction of deoxyartemisnin with receptor protein	45
4.21	Interaction of artemetin with receptor protein	45
4.22	Interaction of casticin with receptor protein	46
4.23	Interaction of sitogluside at cavity 1 with receptor protein	46
4.24	Interaction of sitogluside at cavity 4 with receptor protein	47
4.25	Interaction of beta-sitosterol with receptor protein	47
4.26	Interaction of dihydroartemisinin with receptor protein	48
4.27	Interaction of scopolin with receptor protein	48
4.28	Interaction of artemether with receptor protein	49
4.29	Interaction of artemotil with receptor protein	49

4.30 Interaction of artesunate with receptor protein	50
4.31 Interaction of azithromycin with the receptor	77
4.32 Interaction of chrysopenetin with receptor	78

List of Tables

2.1	Plant compounds and their activity [37, 39].	12
4.1	Physical Properties of M^{pro}	24
4.2	Selected ligands with structural information	26
4.3	Applicability of Lipinski Rule on the Ligands	29
4.4	Toxicity values of selected ligand and standard drug	31
4.5	Docking results of selected ligands	34
4.6	Active ligand showing hydrogen and hydrophobic interactions	50
4.7	Absorption properties of selected ligands and standard drug	60
4.8	Distribution of selected ligands and standard drug.	63
4.9	Metabolic properties of selected ligands and standard drug	65
4.10	Excretion of selected ligands and standard drug	68
4.11	Docking results of Azithromycin	71
4.12	Lipinski Rule Comparison	71
4.13	Toxicity Properties Comparison	72
4.14	Absorption Properties Comparison	73
4.15	Metabolic Properties Comparison	74
4.16	Distribution Properties Comparison	75
4.17	Excretion Properties Comparison	76
4.18	Physiochemical Properties Comparison	76
4.19	Docking Score Comparison	77
4.20	Docking Analysis Comparison	79

Abbreviations

<i>A. annua</i>	<i>Artemisia annua</i>
ACE	Angiotensin-converting enzyme
BBB	Blood-brain barrier
CNS	Central nervous system
FDA	Food drug authority
M ^{pro}	Main protease
MRTD	Maximum rate tolerated dose
OCT	Organic cation transporter
PDB	Protein data bank
RNA	Ribonucleic acid
SARS	Severe acute respiratory syndrome
VD _{ss}	Volume distribution

Chapter 1

Introduction

In 2019 the whole world has faced health crises due to coronavirus which emerged in Wuhan, China, and then was transmitted to the rest of the world. This novel coronavirus termed 2019-nCoV or as severe acute respiratory disease 2 (SARS-CoV-2) first emerged in bats and then was transmitted to humans with intermediary animal sources which are still unknown [1]. The virus belongs to the β -group and is a positive-sense RNA virus and is an enveloped and non-segmented virus. Being an RNA virus SARS-CoV2 has a potential risk for mutations but this rate is much lower in 2019-nCoV than other coronaviruses. The reason is due to its genome encoded exonuclease and with this, the zoonotic virus can easily adapt and become more virulent with its human to human transmission [2]. Coronavirus ranges from 65-125 nm in diameter. SARS-CoV2 has four main structural proteins which include the spike glycoprotein, membrane glycoprotein, small envelope glycoprotein, and nucleocapsid protein with several other proteins [3]. People being affected by this virulent showed symptom like fever, headache, muscle pain, cough, loss of individual's taste or smell sense with sore throat infections. The symptoms appear mostly after 2 to 14 days after being affected. The intensity of infection varies from person to person with mild fever and cough to an intense lung infection, due to this, emergency arises which includes difficulty in breathing [4].

For the life cycle of this virus in the cell, two main polypeptides which are pp1a and pp1ab are required. Both of these proteins are presumed to be processed into

15 nonstructural proteins with the help of two main proteases one is a papain-like protease and the other is the main protease (M^{pro}). This M^{pro} is also termed as the $3CL^{pro}$ and as CL-like protease [5]. This main protease is held responsible for the cleavage at 11 sites in the replicase protease. With this cleavage, certain viral enzymes are released which help the virus to replicate itself. Thus due to this major role played by M^{pro} , it has been selected as a potential target for the development of a drug against Covid-19 [6].

Many vaccines have been developed and each vaccine has a different treatment regime to prevent and minimize the effect of this virus. Different vaccination strategies have to be adopted keeping in mind the demographic regions, the transmission of the virus, and mutations of the virus [7, 8]. Keeping in mind the new strategies for further medicinal development against the coronavirus many of the natural compounds that have previously shown strong antiviral and anti-inflammatory properties have been studied. M^{pro} being a potential drug target has shown effective binding affinity against certain antiviral and anti-inflammatory compounds. For the past three decades' certain computer-assisted drug discovery and drug design methods have been in use that has helped in the development of therapeutic medicines [9]. For this Computational methods such as molecular docking has been in use which can save expenditures, with shortening the time of identifying the potential drug candidates and are faster than manual methods [9].

With the outbreak of Coronavirus in December-2019 in China, in different regions of the world, many herbal treatments were used to treat the symptoms of the spread disease. For controlling and treating the disease various strategies were developed by the research groups, which includes republishing the positive effects of already used medicines and natural products for a fight against Covid-19 [9]. Medicinal plants have been previously used to combat several other viral diseases. Attempts have been made to identify small molecules extracted from the plants that show inhibitory activity against the virus. The genome sequence has identified that SARS-CoV is very similar to the SARS-CoV-2 as $3CL^{pro}$ has been proven a potential target site in SARS-CoV, so for Covid-19 main protease is the target site used for screening against the active compounds of the medicinal plants [10].

One of the plant that has been in talk is *Artemisia annua* which has been found effective against SARS-CoV and now is thought to be active against SARS-CoV 2 also [11]. Although the plant is in clinical trials but still the active constituents of *Artemisia annua* against Covid-19 has to be identified [12].

1.1 Problem Statement

SARS-CoV-2 is a major threat to mankind so we need to discover and identify new compounds with anti-viral properties. This compound should be available frequently and should have least side effects. Due to its role in replication M^{pro} has been identified as a potential drug target. So in this study M^{pro} will be targeted against the active constituents present in *Artemisia annua*.

1.2 Aim and Objectives of Study

The main aim of this study is to screen out the potential inhibitors against SARS-CoV-2 by the use of molecular docking of active compounds of *Artemisia annua* showing antiviral properties with M^{pro} of SARS-CoV-2. The objectives of the study include:

1. To identify the active metabolites present in *Artemisia annua* that have shown antiviral properties.
2. To analyze the interaction between ligand and protein complex by performing molecular docking.
3. To screen out the lead compound on the basis of Lipinski's Rule and ligand ADMET properties.
4. To compare the lead compound with the control to find the best interacting compound against M^{pro}.

Chapter 2

Literature Review

2.1 SARS COV-2

The WHO on February 12, 2020, declared the 2019-nCoV permanently as Severe Acute Respiratory Syndrome Coronavirus 2 causing the disease coronavirus. Coronavirus is a positive-sense RNA virus possessing a large genome. Homology models have shown that the genomic organization of SARS-Cov-2 is similar to the other beta coronaviruses, consisting of the untranslated region at the 5' end, a complex of nonstructural proteins, spike protein gene (S), an envelope protein (E), membrane protein (M) and nucleocapsid protein gene (N) with untranslated regions at the 3' end. The three proteins which are M, E, and S are involved in the viral coat whereas the N protein is held responsible for the packaging of the viral genome (Figure 2.1) [13].

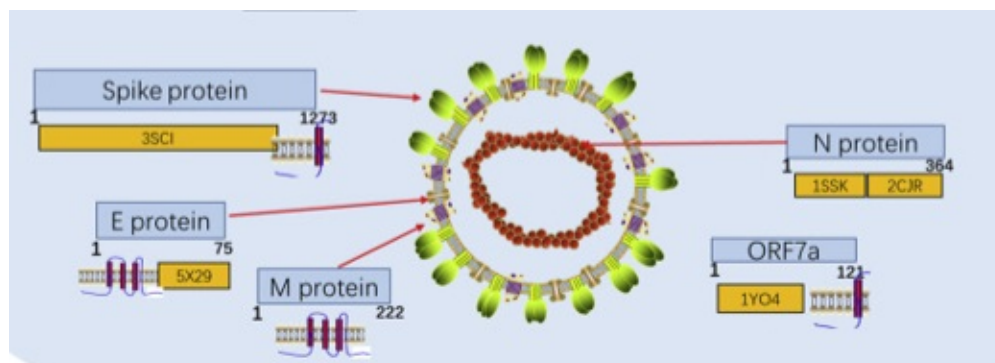


FIGURE 2.1: Structure of SARS-CoV-2 [13].

The virus has not only affected the elderly but young individuals have also been targeted with an increased transmission rate causing several deaths among people. Due to the current pandemic, the human race has been in a great crisis facing several problems both socially and economically [14].

2.2 Origin

With the emergence of the human SARS Coronavirus 2 many questions related to its evolution, the introduction of the virus in the human race, reservoirs of the virus, the spread of the virus, and the linkage of the animal virus with their effects on humans and certain other matters were raised. After obtaining the genomic sequence of the virus it was aligned with the available data in databases with the use of BLASTn to find the homology of this virus. Among the 22 coronaviruses the 3 coronaviruses from the bat including 96% similarity with Bat-CoV Ra TG13 and 88% similarity with bat-SL-CoVZXC12 and bat-SL-CoVZXC45 as in Figure 2.2 [15].

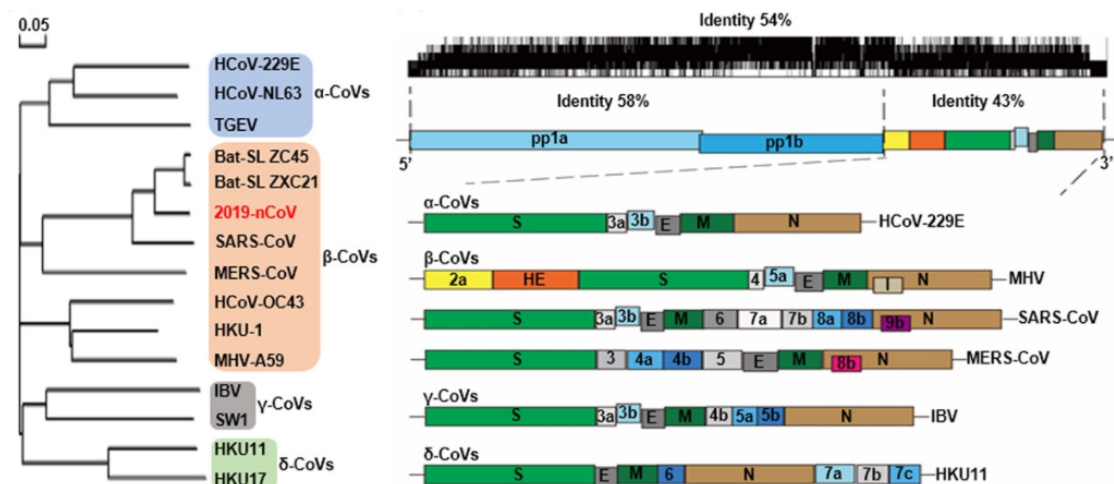


FIGURE 2.2: Sequence alignment of 22 Corona Viruses [15].

The first article published on 21st January about nCoV-19 showed that despite having sequence identity with bat coronavirus the spike protein of the virus interacts in a much stronger way with the ACE2 human receptor [16]. Upon transcription, the beta coronaviruses produce almost 800KD polypeptide. The polypeptide

is cleaved by papain-like protease and 3-chymotrypsin like protease to generate various non-structural proteins involved in viral replication [17].

2.3 Entry and Life Cycle

CRISPR-based screening has been used to study the entry and the life cycle of the SARS-CoV-2 virus. Starting with the attachment of the virus to the cell surface, several genes regulate the biosynthesis of the GAGs (glycosaminoglycan) and the receptor ACE2-a proteinaceous receptor. This receptor is found in various organs of the body like the kidney, heart, lungs, and GI tract.

Endosomal cathepsins L helps in cleaving and the activation of the spike protein of the virus so that it can easily fuse with the ACE2 receptor found in various human organs. A serine proteinase TMPRSS2 present on the plasma membrane facilitates the virus entry in the cell through direct fusion [18].

Next, the protein TMEM41B changes the shape of ER membrane into such pockets which can act as factories for the viral replication as in Figure 2.3. The further process through which the corona virus leaves the infected cell is still not completely understood [19].

After the virus enters the cell, it synthesizes two polyproteins pp1a and pp1ab having a molecular weight of 486 and 790 kDa. During the life cycle of the virus, these two proteins are processed by two proteases to form 15 different non-structural proteins.

The two proteases are papain-like protease and the main protease. The main protease (M^{pro}) is held responsible for cleaving almost 11 sites in the replicase polyprotein that further forms enzymes. The enzymes formed to play a part in the replication of the virus which includes the helicase and the RNA-dependent RNA polymerases. The main protease having an essential role in the replication severs as a drug target site [5, 6].

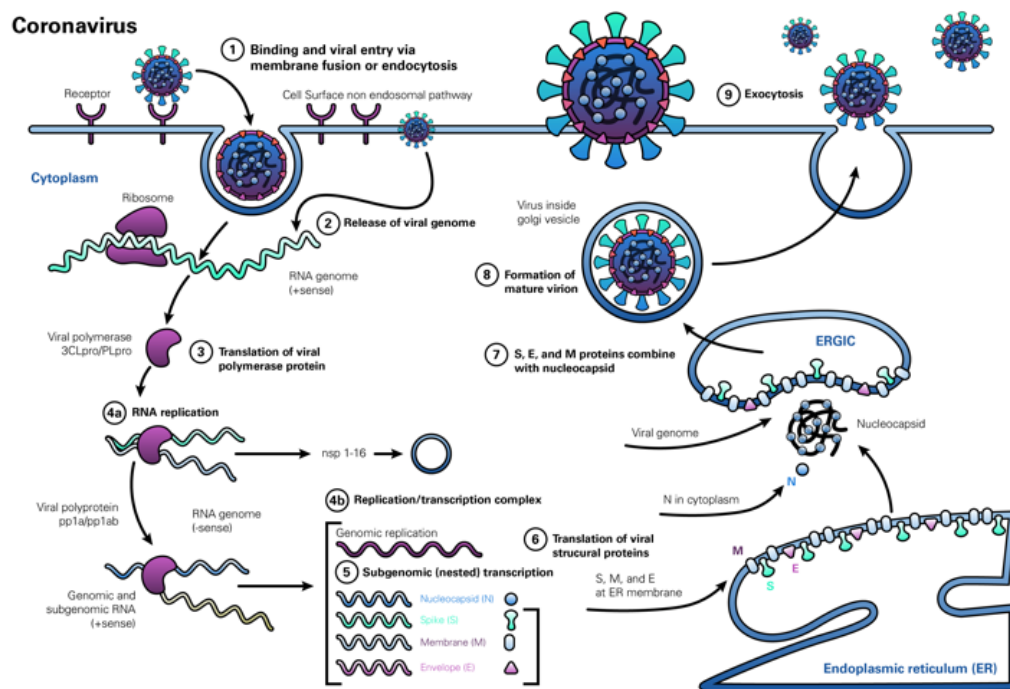


FIGURE 2.3: Entry and life cycle of the SARS-CoV-2 in the human cell [19].

2.4 Symptoms

The SARS-CoV2 affected individuals showed a variation in the symptoms and the rate of infection from acute to severe illness. Approximately 40% of the reactions show asymptomatic infections which showed that these individuals easily reached the recovery phases whereas the fatality rate reached was approximately 1-2% [20]. The human corona virus was a major cause of the upper respiratory tract infections causing the common cold [21]. Studies showed that the novel coronavirus caused severe acute respiratory syndrome that spread from its origin which is China to different regions of the world. An initial study related to the symptoms of the disease showed that almost 91% of individuals showed high fever, 77% had a cough, 44% of individuals faced fatigue. Other symptoms which include salivation was showed by 28%, the headache was common among 8% of people, 5% and 3% showed hemoptysis and diarrhea respectively. Lymphocytopenia was also observed among few individuals. All the infected individuals showed common symptoms of pneumonia and respiratory syndromes at the primary level with 10% of the patients showing a secondary level infection [22].

2.5 Treatment for Corona Virus

To this date, four kinds of vaccine have been developed which includes

1. The whole virus vaccine is developed by using the dead or an inactivated form of the original virus. This vaccine has been developed by Bharat Biotech, Sinovac, and the Wuhan Institute of Biological Products. Sinovac and Sinopharm are the whole virus vaccines [23].
2. The second vaccine developed is of the type of recombinant protein subunit vaccine which targets the spike protein. The vaccine is developed to produce a strong immune response against the virus by attacking the spike protein. By using the nanoparticles technique Novavax is the company to formulate it [23].
3. The third is the replication-incompetent vector vaccine that involves an adenovirus that is weakened and can cause the common cold for a strong immune response. Cansino and Astrazenca are replication incompetent vector vaccine [23].
4. The fourth one is the nucleic (mRNA) based vaccine. The mRNA that produces the spike protein of the virus is injected so that the human immune system forms antibodies against it to protect against the virus. Pfizer, Moderna, and BioNTech have developed a vaccine of this sort [23].

The people being injected with the vaccine has also reported side effects which include pain and swelling at the site of injection, fatigue, mild to severe fever, and headache [23]. For a different kind of vaccine, the dosing strategies also vary, and with each phase of dose, the symptoms may be even more severe.

In European Union, the mRNA-1273 vaccine was injected based on a one-dose-fits-all approach with the elderly having a full dose of the vaccine and the young individual having a half dose of the vaccine. Due to the vaccine injection, the death rate was reduced but the side effects vary from individual to individual [8].

Many drugs were also repurposed that can target M^{pro} protein of the virus. In silico studies were carried on FDA approved drugs such as darunavir, nelfinavir and saquinavir and rosuvastatin [24]. Other drugs include azithromycin, amoxicillin, ceftazidime, moxifloxacin [25].

Out of these azithromycin has been commonly used in Pakistan and in other countries. Azithromycin being a macrolide antibiotic helps in the inhibition of the bacterial proteins, in quorum sensing, and the reduction of biofilm production. Azithromycin is used during respiratory, urinary, dermal, and other bacterial infections. It is also used during chronic inflammatory disorders that include diffuse pan bronchiolitis, post-transplant bronchiolitis, and rosacea [26].

The mechanism of action of azithromycin, supports a large spectrum antiviral activity. It decreases the virus entry into the cells. It helps in regulating, production of interferons type I and III and also the genes which are involved in virus recognition. This is the universal innate response, against the viral infectious and potentially against SARS-CoV-2 [27-29]. Azithromycin also decreases the production of IL-1 β , IL-6, IL-8, IL-10, IL-12 [30]. Seeing the activity of azithromycin it is used as a control in this study.

2.6 Medicinal Plants

Medicinal plants are those that have shown therapeutic properties and have shown beneficial results on humans and animals. Medicinal plants have been used from early times for the treatment of different diseases. In early times with their instincts, taste, and smell ability humans used different plants. Some plants were directly applied to injuries; some were boiled to extract the components present in that plant for treatment. For this, the therapeutic properties of many plants have been under consideration and these plants have been used as an important source for lead drugs [31].

With the outbreak of coronavirus in December 2019 in China, various herbal remedies traditionally used were considered positive for the treatment of nCov-2

affected patients [32]. The plants that were used against Covid-19 were *Pimpinella anisum*, *Curcuma xanthorrhiza*, *Allium sativum*, *Zingiber officinale*, *Allium cepa* and *Olea europaea* [33]. Many of these plants have shown positive result but some of these plants contain toxic substances that could result in intoxications and disorders [33]. For this reason, *Artemisia annua* is exploited for combating the challenge of Covid-19.

2.7 *Artemisia annua*

Artemisia is the largest of the genera included in the family Asteraceae. The name *Artemisia* has been derived from the name of Greek Goddess Artemis who was considered the Protector of the wild. Another proposition about the name of the genus is from the name of the queen (*Artemisia*) of Cairo. The 500 species of this genus are spread all over the world except the extreme colds of Antarctica [34]. Out of the 500 species *Artemisia annua* also named as annual absinthe is an herbaceous plant as shown in Figure 2.4. This plant is majorly grown in Asia and Central and eastern parts of Europe and is also grown in the region of Africa and America [35]. This medicinal plant has been already in use as a part of dietary spice and as herbal tea.

Artemisia annua has been used as a medicinal plant from the late centuries. For the past five decades, this herb is used to act against malaria and other fevers. With this *Artemisia annua* has also shown positive effects as an anti-plasmodium, antiviral, antimicrobial, anti-cholesteric, anti-hyperlipidemic, anti-convulsant, and anti-inflammatory [36]. *Artemisia annua* is rich in approximately 600 active metabolites out of which Artemisinin and its derivatives are most common in use. Other metabolites such as terpenoids, sesquiterpenoids, monoterpenoids, coumarins, flavonoids, alkaloids, triterpenoids, steroids, benzenoids, and alkaloids are also of major interest [37].

Due to the presence of large metabolites, *Artemisia annua* has also shown anti-fungal, antitumor, hepatoprotective, anti-asthmatic, and antioxidants properties.

The plant is also rich in minerals, vitamins and essential amino acids making it an essential candidate for food, pharmaceutical, nutraceutical, medical and cosmetic industries [37]. In Madagascar, a drink was prepared with an infusion of *Artemisia annua* with some other plants to cure Covid-19, but still, studies have to be made to check the toxicity and any sort of harmful effects of the plant in use [38].



FIGURE 2.4: *Artemisia annua* [35].

2.8 Taxonomic Hierarchy

Artemisia annua is the binomial name of the plant belonging to the Asteraceae family. The growing period of the plant is almost 190 to 240 days. It is widely distributed in different regions of the world except in Antarctica [35]. *Artemisia annua* belongs to the kingdom-Plantae, Clade-Traceophytes, Clade-Angiosperms, Clade-Eudicots, Clade-Asterids, Order-Asterales, Family-Asteraceae, Genus-Artemisia and Specie *A. annua* [35].

2.9 Active Constituents of *Artemisia annua*

There are different active constituents present in *Artemisia annua* which are approximately 600 in number. Different class of compounds are present which includes terpenes, monoterpenes, monoterpenoids, flavonoids, sesquiterpenes, phenolic compounds, steroid derivatives, umbelliferone, coumarins and artemisinin derivatives [37, 39].

TABLE 2.1: Plant compounds and their activity [37, 39].

S.No	Compounds	Activity
1	1,8-cineole	Antifungal, anti-inflammatory, antitumor, antibacterial and insecticidal
2	α -pinene	Antimicrobial, anti-inflammatory and a food additive.
3	β -pinene	Antimicrobial, anti-inflammatory and a food additive.
4	camphene	Antitumor, insecticidal, antigastriculer and antifungal
5	borneol	Analgesic and neuroprotective
6	camphor	Anti-estrogenic, uterotrophic, nicotine receptor blocker and a food additive
7	carvone	antimicrobial, anticarcinogenic, immunodialater, antihypertensive
8	limonene	act against angiogenesis
9	α -terpene	Antioxidant
10	myrtenol	protects against lung diseases and is anti-inflammatory
11	artemisinin	antiviral, antiparasitic, antimalarial, antifibrotic, and anti-inflammatory.
12	arteannunin b	antitumor, larvicidal and antiviral
13	artemisnic acid	Antiviral

14	quinic acid	antioxidant, anti-obese, antiviral, inhibitor of glucose 6-phosphate.
15	caffeic acid	Antimicrobial, antiviral, anti-Alzheimer, diabetes and cardiac protector
16	luteolin	Nervous system protector and is an antitumor.
17	quercetin	Antiviral, vasodilator and antioxidant.
18	rutin	Neuro protector, antiviral, antioxidant, antitumor and antidiabetic
19	apigenin	Antimicrobial and antitumor
20	isorhamnetin	antitumor, antidiabetic and anti-inflammatory
21	kaempferol	antitumor and anti-inflammatory
22	mearnsetin	antioxidant.
23	artemetin	antimicrobial, hypotensive and anti-inflammatory
24	casticin	antiaging, antitumor and antioxidant
25	chrysoplenetin	Antiviral.
26	chrysoprenol D	Antitumor, anti-inflammatory and antioxidant.
27	cirsilineol	Antitumor and immunosuppressive
28	eupatorine	Antitumor
29	scopolin	Antioxidant, antiallergic, anti-inflammatory and antimicrobial
30	scopoletin	Antioxidant, antiallergic, anti-inflammatory and antimicrobial

2.10 Molecular Docking

Molecular docking has been in use for the past three decades for designing the drug through computer assistance and to find different structures in molecular biology.

Docking is preferred while performing virtual screening on the compounds present in the databases or libraries for analysis of their functions, results can be classified easily through docking and one of the main roles played by docking is to give the analysis of how the ligand interacted with the protein, locking it for optimizing the lead compounds for drug development [40].

Different docking programs use either one or more search algorithms for the prediction of possible results of the receptor-ligand complex. This is the core reason for molecular docking to become a key tool for drug discovery and molecular modeling applications. The docking result gives a score of the interaction and the accuracy of the scoring function makes docking more reliable for predicting the ligand pose and through that the binding site of the ligand can also be determined. With this, it predicts the binding affiliation which in turn leads to the identification of a potential lead drug in association with the target protein [41].

2.11 3CL Protease

3CL protease or the main protease M^{pro} is an important protease in coronavirus because of its cleaving activity. As it cleaves the 1ab a replicase polyprotein at 11 different sites hence is considered an important enzymatic target to develop drugs against it. The crystallic structure of the SARS-CoV2 M^{pro} was reported which was linked with an N3 inhibitor with a PDB ID as 6LU7 [40]. This protease is considered a cysteine protease as it has a cysteine histidine catalytic dyad and cleaves peptide bond at Gln-Ser/Ala/Gly [42].

In SARS-CoV-2 14 different proteolytic sites of PLpro and 3CLpro were determined by aligning the sequence of amino acids. At the N-terminal, PLpro cleaved three sites at 181-182, 818-819, and 2763-2764, and at the C-terminal 3CLpro cleaved at 11 different sites and produced almost 15 non-structural proteins. These contain Nsp3 with multiple domains with the unique domain of SARS, a proteolytic enzyme, and a deubiquitination enzyme. Nsp5 is the 3CLpro, Nsp12 is RdRp (RNA-dependent-RNA-polymerase) and Nsp13 is a helicase [43].

Three crystal structures of 3CLpro have been reported which are wild-type active dimer, Monomeric forms which cannot dimerize that include G11A, S139A, and R298A mutants and the third type is the highly active dimer. The residues from 8 to 184 are the catalytic domain, the residues from 1 to 18 are the N-terminal finger, and residues from 201 to 306 are the C-terminal domain [43].

2.12 Natural Compounds as Inhibitors of 3CL Protease

The main protease (M^{pro}) of the virus which controls the replication process is considered an active site for targeting the drugs against the virus. The 3D structure of the enzyme is screened against the medicinal plant library with almost 32,297 phytochemicals that have shown antiviral properties. Three drugs Colistin, Nel-finavir, and Prulifloxacin were shown to inhibit the enzyme by drug repurposing strategies. With that certain phytochemicals like 5,7,3',4'-tetrahydroxy-2'-(3,3-dimethylallyl) which is a flavone have shown the highest docking score against M^{pro} . This flavone is extracted from *Psoralea argyrea*, Myricithin from the plant *Myrica cerifera*, Methyl rosmarininate from the plant *Hyptis atrorubens*, 3,5,7,3',4',5'-hexahydroxy flavanone-3-O-Beta-D-glucopyranoside from the plant *Phaseolus vulgaris*, Licoleafol from plant *Glycyrrhiza uralensis*, and Amaranthin from plant *Amaranthus tricolor* were identified as inhibitors to M^{pro} [44].

From tetra peptide inhibitor, 3 serine derivatives were also screened for inhibitory effects. Herbacetin, pectolarin, and rhoifolin were also found to show inhibitory effects. Certain chalcones in alkylated form derived from *Angelica Keiskei* showed inhibition effects. The docking results showed that hydroxyl and carbonyl groups formed hydrogen bonds with Ser-144 and His-163 [45]. In the natural product database, certain compounds were also found to work against 3CLpro and these include compounds like 1-formamido, 6-methyldihydrofuran which were andrographodile derivatives, beutonal which is derived from the plant *Cassine xylocarpa*, Isodecortinol, Cerevistinol both are derived from the plant *Viola diffusa*. Many

other natural compounds from the plants like *Citrus aurantine*, *Scutellin baiclen-sis*, *Phyllanthus emblica*, *Ficus Benjamina*, *Camellia sinensis*, *Swertia kouitchensis*, *Gnidia lamprantha*, *Swertia macrosperma*, and many more plant derivatives have shown promising antiviral, anti-inflammatory activity against the main protease of Covid-19 in *insilico* studies [46].

2.13 Bioactive constituents of *Artemisia annua*

There is a large number of naturally occurring compounds that can serve as antivirals to inhibit the activity of the main protease of SARS-CoV2 [46]. The plant *Artemisia annua* has been used from earlier times either in the form of tea or in the form of juice for curing of malaria and other fevers. This was such a remarkable cure that this herb approximately 4.5-5g in dried weight was converted into an infusion for clinical trials [39].

Different metabolic compounds are obtained from the roots, oil, and leaves of the plant which include terpenes, monoterpenes, polyphenols, flavonoids, Coumarins, and sesquiterpenoids [37]. A drink based on the infusion of *Artemisia annua* with other plants was used in Madagascar for a cure to Covid-19. But still, the role of the plant against the virus has to be studied [39]. For this reason the active constituents against Covid-19 in *Artemisia annua* has to be screened out.

Chapter 3

Materials And Methods

3.1 Selection of Protein

SARS CoV-2 3CLpro, being a part of replicase protein helps in cleaving functional polypeptides, which eventually leads to maturation of SARS-CoV-2. Because of the functional importance, 3CLpro or M^{pro} is a potential drug target site [47]. The structure of SARS-Cov2 M^{pro} was downloaded from the available resource of the protein data bank(PDB). With the DOI 10.2210/pdb6LU7/pdb and the PDB ID 6Glu7, the crystal-like structure of the main protease of covid-19 was downloaded.

3.2 Determination of physiochemical Properties of Proteins

The determination of the physical and chemical properties of a protein play an important role in the finding of its function. ProtParam, a tool of ExPASy was used for this purpose. Physiochemical properties like the molecular weight, isoelectric point, number of amino acids present, grand average of hydropathicity, instability index, number of negatively charged residues (Asp+ Glu), and positively charged residues (Arg+Lys) were studied [48].

3.3 Cleaning of the Downloaded Protein

After downloading the protein structure, the extra constituents attached to the protein need to be removed which was done by the use of an open-source system Pymol. The linear chain of the protein consisted of a range of 1-306 amino acids and was referred to as the A chain and remaining all the constituents of the protein was eliminated so that further process is done effectively [49].

3.4 Determination of Functional Domains of Target Proteins

For determining the domains of the target protein InterPro a database that can analyze a protein was used that, provided information regarding the families, functional sites, and the domains of the protein under study [50]. By inserting the FASTA sequence of the main protease, was obtained the polypeptide binding sites and homodimer interfaces.

3.5 Selection of Active Metabolic Ligands

Selected ligands for the study had previously shown some antiviral and antimalarial properties include compounds from various classes reported from *Artemisia annua* which are terpenes, monoterpenes, sesquiterpenes, phenolic compounds, flavonoids, coumarins, and sterols [37, 39].

3.6 Ligand Preparation

By using the database PubChem, the 3-dimensional structure of the above-selected ligands was downloaded. PubChem is under the National Center of Biotechnology Information (NCBI) and is a database that contains information regarding

the chemical molecules. The information stored is related to the chemical names, molecular formulas. 3 dimensional or simple structures, their isomers, canonical similies, and information regarding the activities of the molecules against the biological assays [51]. The structure of the ligands which were obtained from PubChem were all downloaded and then the ligands MM2 energy was minimized by using Chem3D ultra. In the end, the SDF format was selected to save the structure of energy minimized ligands [51].

3.7 Molecular Docking

For performing the molecular docking between the protein and the ligand, CB-dock (Cavity detection guided blind docking) was used. CB dock finds the sites of docking automatically. CB-Dock is a method of protein and ligand docking that indicates the sites of bonding, the size, and the center is calculated. The box size is adjusted according to the ligand and then docking is performed. The docking was performed through AutoDock Vina.

Docking focus on cavity binding so that ratio of accuracy is higher [52]. For performing the docking, we uploaded the 3D structure of a protein in pdb format and the 3D structure of ligand in the SDF format. After this docking was performed. The result was 5 different poses of interaction. To select the best pose, we looked upon the minimum vina score which was given in KJ/mol [53].

3.8 Visualization of Docking Result via PyMol

Over the past few years, the PyMol has emerged as an efficient molecular tool of visualization. The graphics and its ability to view 3D structures have been extraordinary [49]. PyMol provides a plugin that can access the results and make their visualization clearer so that the docking results can be easily studied. The pictures of the docking result can be captured also [54]. For all the process the

docking result was saved in the pdb format and after visualization in the PyMol was also be saved in the pdb file format.

3.9 Analysis of Docked Complex via LigPlot

Once we get the docked complex with the lowest vina score, the next step was the analysis of the complex. The complex was in the pdb format. This analysis was done by using the software LigPlot. For the given pdb file format the schematic diagrams of the protein and ligand interactions were generated automatically.

These interactions were modified by hydrogen bonds and through hydrophobic contacts. LigPlot provides the analysis of the hydrophobic and hydrogen bonding interactions. LigPlot generates the 2D representation of the protein-ligand complex [55].

3.10 Ligand ADME Properties

After the analysis, the next step was the study of pharmacokinetics and toxicity properties. By using the PkCSM optimization of the ADME which is absorption, distribution, Metabolism, and excretion related to the human body was done [56].

3.11 Lead Compound Identification

To identify the lead compound, Lipinski rule of 5 is used which includes:

1. The log value of the drug-like compound must be limited to 5.
2. The molecular weight should also be lesser than 500.
3. The hydrogen bond acceptor's maximum number should be 10.
4. The hydrogen bond donor's maximum number should be 5.

Once the compound fulfills these rules it was selected as our lead compound. The selected compound is the lead compound [57].

3.12 Comparison with the Standard Drug

Azithromycin, a drug that has been effective against MERS, SARS-Cov, and other microbes has been selected as a standard drug for comparison against the lead compound. Though azithromycin is in use for treatment against covid-19 but frequent use of this drug can lead to antimicrobial resistance [58, 59].

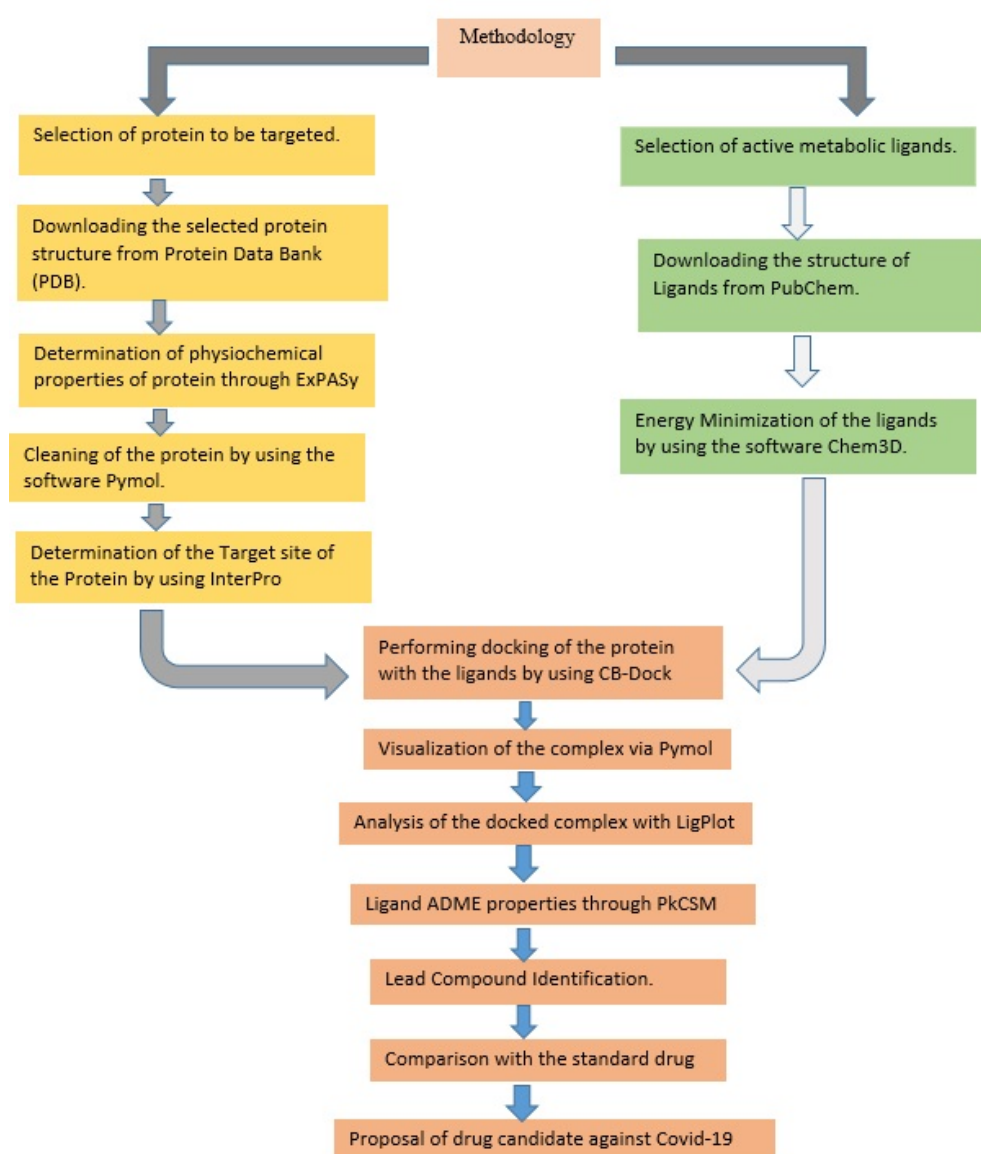


FIGURE 3.1: Methodology opted for this study.

Chapter 4

Results and Discussion

4.1 Structure Modelling

M^{pro} is selected as the target protein to act against the active components present in *Artemisia annua*. The M^{pro} of the SARS-CoV2 plays a major role in the cleavage of 11 sites in replicase polyproteins which releases certain enzymes that are needed for the replication of the virus [47].

4.1.1 3D Structure of the Protein

The protein selected which is M^{pro} is a CoV enzyme, which plays an important role in mediating the replication and transcription of the virus. For this reason it is considered as an attractive enzyme of the virus to be targeted.

M^{pro} is a 33.8 kDa protein which digests the polyprotein at almost 11 conserved sites making it a efficient drug target [60]. The PDB (Protein Data bank) contains a large amount of data regarding the protein-ligand complexes.

The 3D structure of the main protease of coronavirus is obtained from a protein data bank (PDB) named 6LU7 with the DOI 10.2210/pdb6LU7/pdb. The protein obtained is attached with an N3 inhibitor as in Figure 4.1 which needs to be removed for further processing.



FIGURE 4.1: 6LU7 complexed with N3 inhibitor-the red dots show the inhibitor.

4.1.2 Physiochemical Properties of Protein

For studying the properties of protein M^{pro} a tool of ExPASy named as ProtParam is used. It is an online tool that is used for computing the physical and chemical properties of proteins that are entered in the Swiss-prot or TrEMBL or for the proteins entered by the users. The parameters which are studied include the molecular weight, protein's amino acid composition, atomic composition, theoretical pI, estimated half-life, extinction co-efficient, instability index, aliphatic index, and the last is the grand average of hydropathicity (GRAVY) [61].

With this, the protein showing pI greater than 7 means the basic nature of the protein whereas a pI value lesser than 7 indicates the acidic nature of the protein. Extinction coefficient indicates the light absorption whereas instability index represents stability level of protein if it is lesser than 40 then that means the protein is stable any value greater than 40 shows that protein is unstable [62].

The aliphatic index shows the thermo-stability of a protein. The molecular weight (MW) of the protein shows both the positive and the negative amino acid residues. NR indicates the negative residues (Asp+Glu) and PR represents the positive charge residues (Arg+Lys). The low GRAVY value shows the interaction with water molecules. All the above-mentioned parameters were taken into consideration [62].

The physical properties of the selected protein M^{pro} are discussed in Table 4.1

TABLE 4.1: Physical Properties of M^{pro}

MW	pI	NR	PR		
33796.64	5.95	26	22		
Ext. Co 1	Ext. Co 2	Instability Index	Aliphatic Index	GRAVY	
33640	32890	27.65	82.12	-0.019	

The above table shows the molecular weight of M^{pro} as 33796.64 which is a collective weight of negative and positive amino acids residues. The pI is 5.95 which indicates that the selected protein is acidic in nature. The values of light absorption in terms of extinction coefficient is 33640 and 32890. The instability index value of 27.65 shows that selected protein M^{pro} is quite a stable protein. Aliphatic index also shows that selected protein is thermostable. Low value of GRAVY shows that M^{pro} has good interactions with water molecules.

4.1.3 Identification of Functional Domains of the Protein

For identifying the functional domains InterPro consortium is used. InterPro helps in finding the functional analysis of proteins and classifies them into families which is done by finding functional domains and other important sites. Functional domains are the active part of the protein that is used by the protein for interacting with other proteins or other substances. The job ID for finding the functional domain of 6LU7 is <https://www.ebi.ac.uk:443/interpro//result/InterProScan/iprscan5-R20210417-071019-0353-62313319-p2m/>

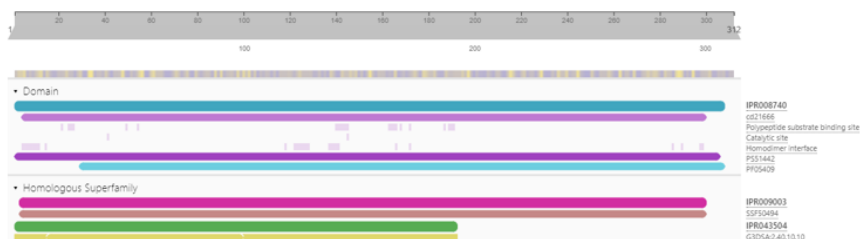


FIGURE 4.2: Functional domains of targeted protein.

Figure 4.2 shows the functional domains of the protein to be targeted. Two protomers A and B combine to form a single polypeptide. It consists of 1-306 residues. Each protomer has 3 domains, Domain I has 8-101 residues whereas Domain II has 102-184 residues. The third domain has got 201-303 residues. The Domain I and II has a cleft which acts as a substrate binding site [60].

4.1.4 Structure of Protein Refined for Docking

The structure of the protein is refined by the use of PyMol. The N3 inhibitor as it inhibits the activity of M^{pro} needs to be removed [60]. The extra side-chain C is also removed as shown in Figure 4.3, now the protein is ready for docking. Domains I and II have an antiparallel β -barrel structure whereas Domain III has a globular cluster which consists of five antiparallel α -helices. Domain III is connected by Domain II by a loop region consisting of 185-200 residues [60].

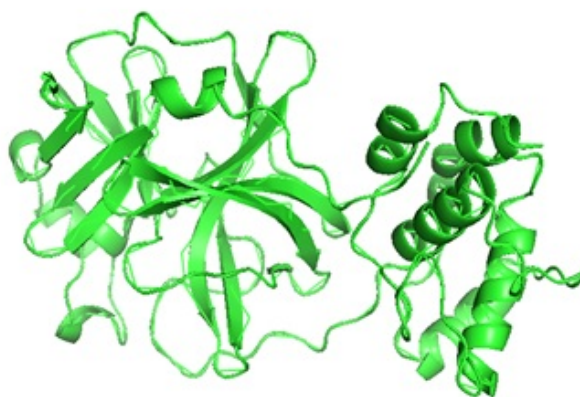


FIGURE 4.3: 6LU7 cleaned protein

4.2 Ligand Selection



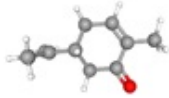
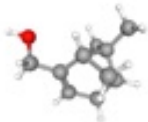
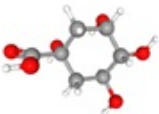
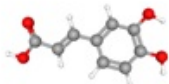
The ligand selected is based on the best resolution structure based on the chemical class of the crystal bounded to the protein and then based on their binding affinities. What matters is the conformational selection of the ligand. This selection is a process where a ligand binds selectively to one of the conformers, strengthens it,

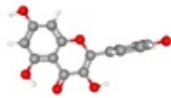
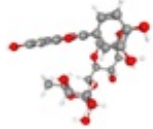
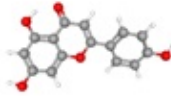
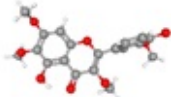
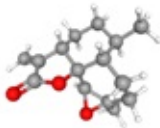
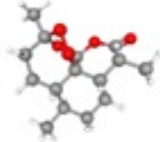
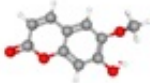
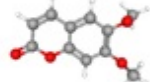
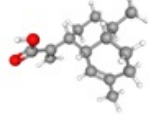
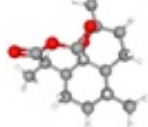
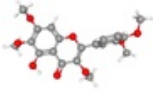
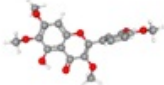
and increases its population with respect to the total population of that protein [35-39].

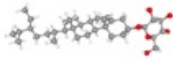
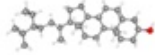
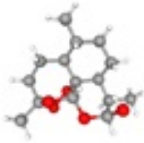
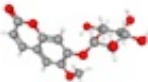
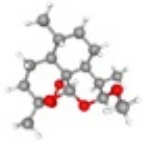
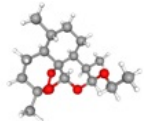
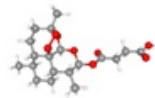
The ligands which are the active constituents of the selected plant were searched from the world's largest chemical databank- PubChem. The 3D structures of these ligands were downloaded from PubChem in the SDF format. Table 4.2 shows all the selected ligands with the information regarding their structure [35-39].

After downloading the structures of the ligands that were selected the next step that was performed was minimizing the energy of these ligands. This step is an important one as we can't use simply the downloaded structure as the ligands are unstable and it can directly affect the docking vina scores.

TABLE 4.2: Selected ligands with structural information

S No.	Ligand Name	Molecular Formula	Molecular Weight g/mol	Structure
1.	alpha-pinene	C ₁₀ H ₁₆	136.23	
2.	beta pinene	C ₁₀ H ₁₆	136.23	
3.	Carvone	C ₁₀ H ₁₄ O	150.22	
4.	Myrtenol	C ₁₀ H ₁₆ O	152.23	
5.	Quinic acid	C ₇ H ₁₂ O ₆	192.17	
6.	Caffeic acid	C ₉ H ₈ O ₄	180.16	

7.	Quercetin	$C_{15}H_{10}O_7$	302.23	
8.	Rutin	$C_{27}H_{30}O_{16}$	610.5	
9.	Apigenin	$C_{15}H_{10}O_5$	270.24	
10.	chrysopenetin	$C_{19}H_{18}O_8$	374.3	
11.	Arteannunin b	$C_{15}H_{20}O_3$	248.32	
12.	artemisinin	$C_{15}H_{22}O_5$	282.33	
13.	Scopoletin	$C_{10}H_8O_4$	192.17	
14.	Scoparone	$C_{11}H_{10}O_4$	206.19	
15.	Artemisnic acid	$C_{15}H_{22}O_2$	234.33	
16.	Deoxyartemisnin	$C_{15}H_{22}O_4$	266.33	
17.	Artemetin	$C_{20}H_{20}O_8$	388.4	
18.	Casticin	$C_{19}H_{18}O_8$	374.3	

19.	Sitogluside	$C_{35}H_{60}O_6$	576.8	
20.	beta sitosterol	$C_{29}H_{50}O$	414.7	
21.	Dihydroartemisnin	$C_{15}H_{24}O_5$	284.35	
22.	Scopolin	$C_{16}H_{18}O_9$	354.31	
23.	Artemether	$C_{16}H_{26}O_5$	298.37	
24.	Artemotil	$C_{17}H_{28}O_5$	312.4	
25.	Artesunate	$C_{19}H_{28}O_8$	384.4	

4.3 Virtual Screening and Toxicity Prediction through Lipinski Rule of Five

For compounds to be separated as drug-like and non-drug-like Lipinski rule of five and ADME properties are followed [56, 57]. The Lipinski rule deals with certain parameters like Molecular weight which should be ≤ 500 , $\log P \leq 5$, H-bond donors ≤ 5 , H-bond acceptors ≤ 10 .

These rules are to be followed by orally active compounds. The drug-like is dependent on the mode of administration [57]. A compound is considered a drug when it follows 3 or more rules and if a compound violates two or more rules it is considered poorly absorbed [57]. Table 4.3 gives the value of Lipinski Rule for the selected ligands.

TABLE 4.3: Applicability of Lipinski Rule on the Ligands

S. No	Ligand	Log P-value	Molecular Weight g/mol	H-bond Acceptor	H-bond Donor
1.	Alpha-pinene	2.9987	136.23	0	0
2.	Beta pinene	2.9987	136.23	0	0
3.	Carvone	2.4879	150.22	1	0
4.	Myrtenol	1.9711	152.23	1	1
5.	Quinic acid	-2.3214	192.17	5	5
6.	Caffeic acid	1.1956	180.16	3	3
7.	Quercetin	1.988	302.23	7	5
8.	Rutin	-1.6871	610.5	16	10
9.	Apigenin	2.5768	270.24	5	3
10.	Chrysopenetin	2.9056	374.3	8	2
11.	Arteannunin b	2.4518	248.32	3	0
12.	Artemisinin	2.3949	282.33	5	0
13.	Scopoletin	1.5072	192.17	4	1
14.	Scoparone	1.8102	206.19	4	0
15.	Artemisnic acid	3.6458	234.33	1	1
16.	Deoxyartemisnin	2.4633	266.33	4	0
17.	Artemetin	3.2086	388.4	8	1
18.	Casticin	2.9056	374.3	8	2
19.	Sitogluside	5.849	576.8	6	4
20.	Beta-sitosterol	8.0248	414.7	1	1
21.	Dihydroartemisnin	2.1867	284.35	5	1
22.	Scopolin	-1.0197	354.31	9	4
23.	Artemether	2.8408	298.37	5	0
24.	Artemotil	3.2309	312.4	5	0
25.	Artesunate	2.6024	384.4	7	1
26.	Azithromycin	1.9007	748.996	14	5
	(Standard Drug)				

The above table shows that out of the 25 ligands, Rutin does not follow the Lipinski rule at all whereas Sitogluside disobeys two Lipinski rule that are of LogP value and that of molecular weight. Azithromycin being a standard drug does not follow the rule of molecular weight and hydrogen bond acceptor.

4.3.1 Toxicity Prediction

PkCSM is an online tool that is used to predict the values of ADMET (absorption, distribution, metabolism, excretion, and toxicity) of the bioactive compounds and drugs. By using this tool, we will determine the toxicity of the ligands selected, for this different methods are used to test whether a given ligand is toxic or not [63-65]. AMES toxicity test is used to test the mutagenic potential of the compound by using bacteria. If it shows a positive response, then the ligand is mutagenic which can also act as a carcinogen [63-65]. *T. Pyriformis* toxicity method uses *T. Pyriformis* (protozoa bacteria) toxicity as a toxic endpoint. Any value > -0.5 log ug/L is considered toxic [63-65]. The values predicted in the Minnow toxicity test are used to represent the concentration at which the compound could cause the death of 50% of the minnows. The value below 0.5 mM is regarded as acute toxic [63-65]. The values for MRTD (maximum recommended tolerated dose) gives a picture of the starting dose of a certain pharmaceutical at clinical phase I. Value ≤ 0.477 log mg/kg/day is low and a value greater than this value is considered as high [63-65]. For the oral rat chronic test of toxicity, the predicted log value of the lowest observed adverse effect in log mg/kg.bw/day is given which relates to the concentration of the compound given that requires the treatment time [63-65]. A hepatotoxicity test predicts that if a compound could affect the liver functioning or not [63-65]. A skin test predicts whether the compound could give any skin reactions or not [63-65]. The hERG I and II inhibitor test determine the potential of any compound to cause the inhibition of the potassium channels associated with hERG. An inhibitor of these channels could lead to QT syndrome and on a long-term basis the person could develop ventricular arrhythmia [63-65]. The toxicity predicted values of the selected ligands are shown in the Table 4.4

TABLE 4.4: Toxicity values of selected ligand and standard drug

Ligands	AMES Toxicity	Max. tole- rated dose (human)	hERG I inhibitor	hERG II inhibitor	Oral rat acute toxicity	Oral rat chronic toxicity	Hepato- toxicity	Skin sensit- ization	T. pyri- formis toxicity	Minnow toxicity
α -pinene	No	0.48	No	No	1.77	2.262	No	No	0.45	1.159
β -pinene	No	0.371	No	No	1.673	2.28	No	No	0.628	1.012
Carvone	No	0.775	No	No	1.86	1.972	No	Yes	0.41	1.445
Myrtenol	No	0.439	No	No	1.746	1.8	No	Yes	0.262	1.698
Quinic acid	No	1.626	No	No	1.128	3.529	No	No	0.285	4.869
Caffeic acid	No	1.145	No	No	2.383	2.092	No	No	0.293	2.246
Quercetin	No	0.499	No	No	2.471	2.612	No	No	0.288	3.721
Rutin	No	0.452	No	Yes	2.491	3.673	No	No	0.285	7.677
Casticin	No	0.47	No	No	2.302	1.768	No	No	0.317	2.233
Chrysop- lenetin	No	0.491	No	No	2.324	1.773	No	No	0.313	2.248
Apigenin	No	0.328	No	No	2.45	2.298	No	No	0.38	2.432
Artean- nunin b	No	0.195	No	No	2.052	1.589	No	No	0.45	1.53

Artemi- sinic acid	No	0.403	No	No	1.747	2.251	No	Yes	0.541	0.541
Artemisinin	Yes	0.065	No	No	2.459	1	No	No	0.322	1.406
Deoxyar- temisinin	No	0.174	No	No	2.161	1.506	No	No	0.363	1.538
Dihydro- artemisinin	Yes	0.014	No	No	2.227	0.995	No	No	0.298	1.067
Artemetin	No	0.335	No	No	2.36	1.025	No	No	0.332	1.842
Artemether	No	0.074	No	No	2.429	1.043	No	No	0.304	0.587
Artemotil	No	0.019	No	No	2.32	0.952	No	No	0.347	1.799
Artesunate	No	0.256	No	No	3.112	1.549	No	No	0.285	1.499
Scopoletin	No	0.614	No	No	1.95	1.378	No	No	0.516	1.614
Scoparone	No	0.494	No	No	2.345	2.408	No	No	0.603	1.223
Scopolin	No	0.393	No	No	2.391	3.756	No	No	0.286	4.198
Sitogluside	No	-0.887	No	No	2.571	3.293	No	No	0.285	-0.811
Beta-sitosterol	No	-0.621	No	Yes	2.552	0.855	No	No	0.43	-1.802
Azithromycin	No	1.927	No	No	2.769	1.991	Yes	No	0.285	7.8
(Standard Drug)										

The table shows that artemisinin and dihydroartemisinin both are AMES toxic which means that can be mutagenic which can later be carcinogenic. Rutin and beta-sitosterol are hERG II inhibitor that can lead to potassium channel inhibition leading to QT syndrome. Hepatotoxicity test of azithromycin tells that it is toxic to liver. Myrtenol and artemisnic acid are sensitive to skin. The values of *T.pyrifomis* toxicity shows that β -pinene, artemisnic acid and scopoletin are toxic. Sitogluside and beta-sitosterol are minnow toxic.

Toxicity parameters value of Azithromycin shows that this drug can be toxic towards liver but other parameters are in the range of positive values. Azithromycin can not cause any sensitivity to skin and it also not an inhibitor of hERG I and hERG II. The dose value of 1.927 is also tolerable. With that a no to AMES toxicity indicates that it is not carcinogenic.

4.4 Molecular Docking

Molecular docking is a technique that is used for the estimation of the strength between a ligand bonded to a receptor protein through the vina score function and for determining the correct structure of the ligand that binds to the binding site. The 3D structure of the ligands and the protein are taken to perform docking. For this purpose, CB dock an online blind auto docking tool is used [63, 65].

CB Dock predicts the binding sites of the protein and calculates the cavity sizes. After docking, CB Dock gives us the five best poses and receptor models. Among these five the best pose was selected depending on the vina score and the size of the cavity [64, 65]. Molecular docking is performed by using M^{pro} as the receptor protein and the 25v ligands selected above. The protein is in the PDB format and the ligands are in the SDF format. CB dock then checks the input files and then converts them into pdbqt format files by using OpenBabel and MGL Tools [65].

Then CB dock predicts the cavities of the receptor and also calculates the centers and sizes of the top five cavities. Among the five best conformations the best one is selected based on a high-affinity score of the interaction between the protein

and the ligand [65].Ligands showing the best binding score between the selected ligands and the protein M^{pro} are shown in table 4.5

TABLE 4.5: Docking results of selected ligands

Ligands	Binding Score KJ/mol	Cavity size	H B D	H B A	logP	Mol. Weight g/mol	Rotatable Bonds	Grid Map
α -pinene	-4.8	212	0	0	2.9987	136.23	0	53.705
β -pinene	-4.7	212	0	0	2.9987	136.23	0	53.705
Carvone	-5.1	212	0	1	2.4879	150.22	1	53.705
Myrtenol	-5.2	212	1	1	1.9711	152.23	1	53.705
Quinic acid	-5.4	258	5	5	-2.3214	192.17	1	71.716
Caffeic acid	-6	212	3	3	1.1956	180.16	2	53.705
Quercetin	-7.6	258	5	7	1.988	302.23	1	71.716
Rutin	-8.9	258	10	16	-1.6871	610.5	6	71.716
Casticin	-7.6	258	2	8	2.9056	374.3	5	71.716
Chryso- plenetin	-7.7	258	2	8	2.9056	374.3	5	71.716
Apigenin	-7.8	258	3	5	2.5768	270.24	1	71.716
Artean- nunin b	-6.6	212	0	3	2.4518	248.32	0	53.705
Artemi- sinic acid	-7	212	1	1	3-6458	234.33	2	53.705
Artemisinin	-7	212	0	5	2.3949	282.33	0	53.705
Deoxyar- temisinin	-7.2	258	0	4	2.4633	266.33	0	71.716
Dihydroar- temisinin	-7.1	212	1	5	2.1867	284.35	0	53.705
Artemetin	-7.6	258	1	8	3.2086	388.4	6	71.716
Artemether	-7.1	212	0	5	2.8408	289.37	1	53.705
Artemotil	-7.1	258	0	5	3.2309	312.4	2	71.716
Artesunate	-7.5	258	1	7	2.6024	384.4	4	71.716

Scopoletin	-5.9	212/ 258	1	4	1.5072	192.17	1	53.705/ 71.716
Scoparone	-6	212	0	4	1.8102	206.19	2	53.705
Scopolin	-7.5	258	4	9	-1.0197	354.31	4	71.716
Sitogluside	-7.6	688/ 239	4	6	5.849	576.8	9	56.178/ 58.474
Beta-sito- sterol	-6.9	212	1	1	8.0248	414.7	6	53.705

Table 4.5 shows the docking result of selected ligands and that of azithromycin selected as a standard and also indicates the value of permeability of the drugs in the tissues by logP values. The results shows that the docking score of α -pinene is -4.8 KJ/mol, with not accepting and donating any hydrogen. β -pinene shows the docking score of -4.7 KJ/mol with not accepting or donating any hydrogen, and both gives a logP value of 2.9987 as they are isomers of each other. Carvone shows a binding score of -5.1 KJ/mol. Myrtenol and Quinic acid gives the binding score as -5.2 KJ/mol and -5.4 KJ/mol. Carvone, Myrtenol and Quinic acid gives a logP value of 2.4879, 1.9711 and -2.3214.

Ligands like alpha-pinene, beta-pinene, carvone and myrtenol had already been reported to be docked against the M^{pro} by using Auto dock. α -pinene shows the same binding score of -4.8 KJ/mol as already been reported by P Bhattacharya, TN Patel – 2021 β -pinene show a score of -4.6 KJ/mol in place of -4.7 KJ/mol and carvone show a binding score of -4.8 KJ/mol instead of -5.1 KJ/mol [63]. Myrtenol show a score of -5 KJ/mol in place of -5.2 KJ/mol as reported by Yabrir in 2021 [66].

Rutin shows the binding score of -8.9 KJ/mol and a logP value of -1.6871. Apigenin shows quite a good binding score of -7.8 KJ/mol and a logP value of 2.5768 with that chrysopenetin also shows a binding score of -7.7 KJ/mol and a logP value of 2.9056. After these quercetin shows a score of -7.6 KJ/mol and a logP value of 1.988, caffeic acid has shown a binding score of -6 KJ/mol with a logP value of 1.1956.

Ligands like quercetin, rutin and apigenin had already been reported to be docked against the M^{pro} by using Auto dock wizard. Quercetin shows the binding score of -7.2 KJ/mol which is lesser than the docking score showed by CB-Dock as already been reported by Oluwaseun Taofeek in 2020 [67]. Rutin show a score of -7.7 KJ/mol in place of -8.9 KJ/mol and apigenin show a binding score of -6.8 KJ/mol instead of -7.8 KJ/mol [67].

Artemisinin and artemisnic acid shows the binding score of -7 KJ/mol and a logP value of 2.3949 and 3.6458 respectively. Arteannunin b shows a score of -6.6 KJ/mol and a logP value of 2.4518, scoparone shows a binding score of -6 KJ/mol with a logP value of 1.8102 and scopoletin shows a binding score of -5.9 KJ/mol and a logP value of 1.5072. Artemetin, casticin and sitogluside shows a binding score of -7.6 KJ/mol and logP values as 3.2086, 2.9056 and 5.849, deoxyartemisinin shows the score of -7.2 KJ/mol and a logP value of 2.4633 and beta-sitosterol gives a binding score of -6.9 KJ/mol with a logP value of 8.0248. Dihydroartemisinin, artemether and artemotil shows a binding score of -7.1 KJ/mol with logP values as 2.1867, 2.8408 and 3.2309, and scopolin and artesunate shows the score of -7.5 KJ/mol and logP value of -1.0197 and 2.6024 respectively.

4.5 Interaction of Ligands and Targeted Protein

The result deduced from docking is analyzed through LigPlot and PyMol. The interaction between the Ligands and the receptor protein is predicted through Lig-Plot+. The graphical system of LigPlot automatically generates the 2D pictures of interactions from its 3d coordinates. The 2D pictures display the hydrogen bond interactions and hydrophobic contacts between the ligand and the main chain or side chain elements of the receptor protein [65]. The 2D diagrams of the interaction of the ligands and the protein are shown in figures 4.5-4.30 whereas table 4.19 shows the hydrogen and hydrophobic interactions.

Figure 4.4 shows the interaction of α -pinene with receptor protein M^{pro} . It shows that α -pinene has formed six hydrophobic interactions.

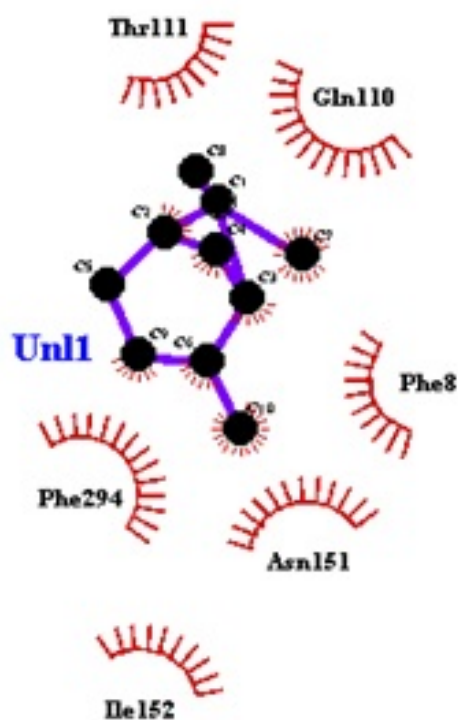


FIGURE 4.4: Interaction of α -pinene with the receptor protein

Figure 4.5 shows the interaction of β -pinene with receptor protein M^{pro} . It shows that β -pinene has formed four hydrophobic interactions.

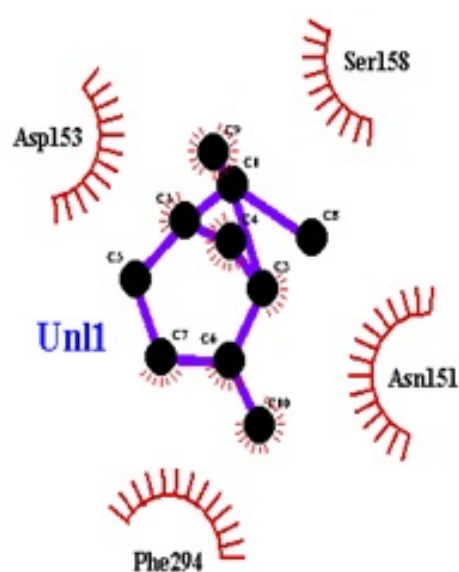


FIGURE 4.5: Interaction of β -pinene with receptor protein

Figure 4.6 shows the interaction of carvone with receptor protein M^{pro} . It shows that carvone has formed six hydrophobic interactions and one hydrogen bond.

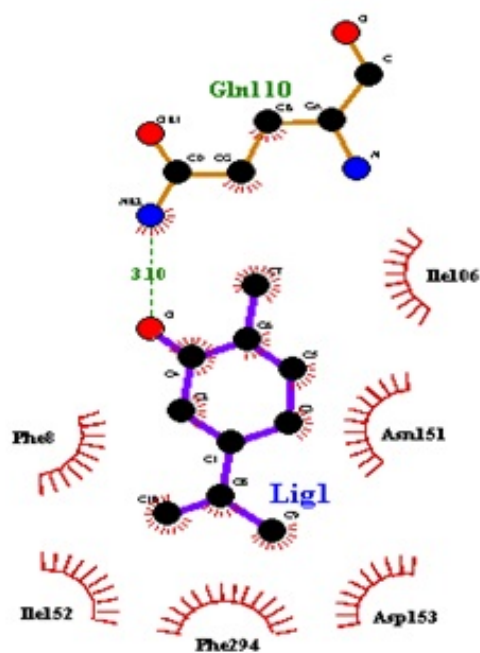


FIGURE 4.6: Interaction of carvone with receptor protein

Figure 4.7 shows the interaction of myrtenol with receptor protein M^{pro} . It shows that myrtenol has formed four hydrophobic interactions and three hydrogen bonds.

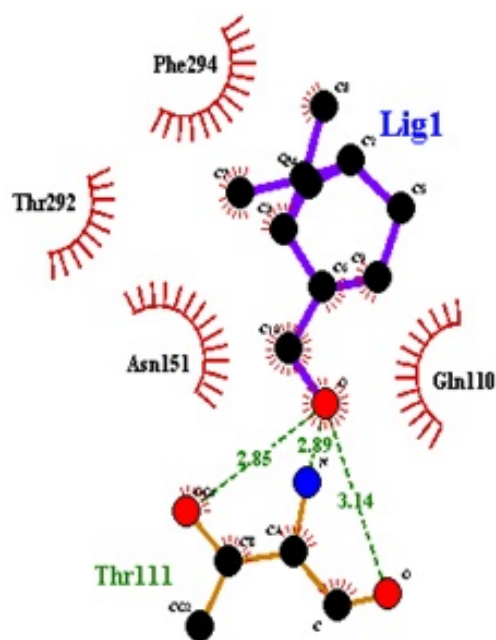


FIGURE 4.7: Interaction of myrtenol with receptor protein

Figure 4.8 shows the interaction of quinic acid with receptor protein M^{pro} . It shows that quinic acid has formed three hydrophobic interactions and ten hydrogen bonds.

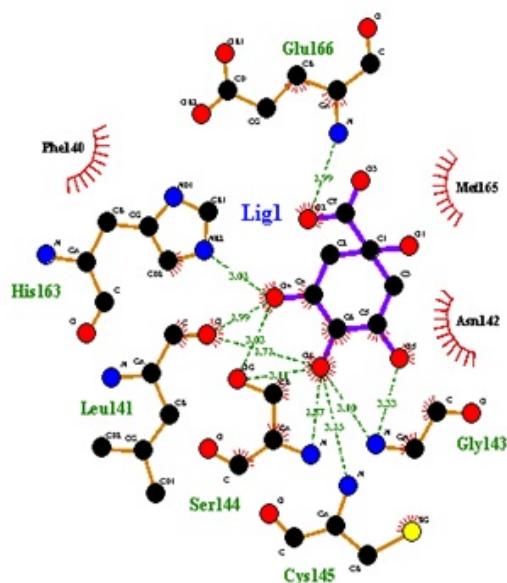


FIGURE 4.8: Interaction of quinic acid with receptor protein

Figure 4.9 shows the interaction of caffeic acid with receptor protein M^{pro} . It shows that caffeic acid has formed five hydrophobic interactions and five hydrogen bonds.

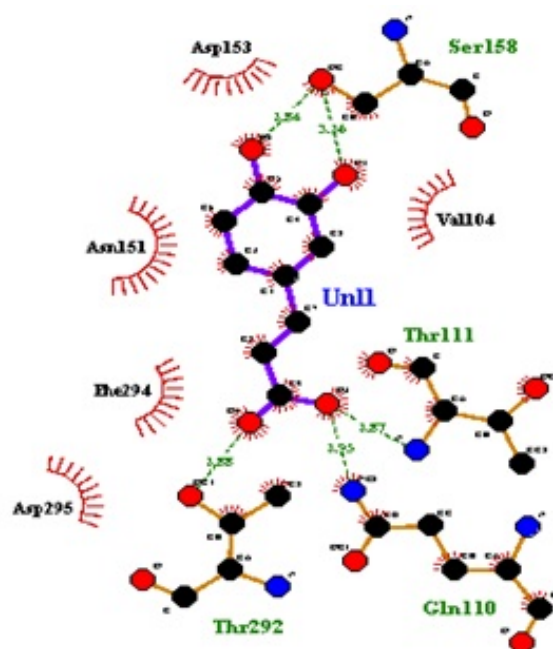


FIGURE 4.9: Interaction of caffeic acid with receptor protein

Figure 4.10 shows the interaction of quercetin with receptor protein M^{pro} . It shows that quercetin has formed nine hydrophobic interactions and two hydrogen bonds.

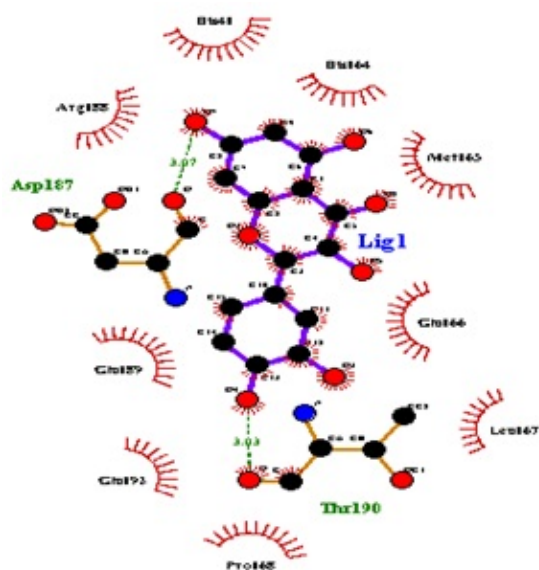


FIGURE 4.10: Interaction of quercetin with receptor protein

Figure 4.11 shows the interaction of rutin with receptor protein M^{pro} . It shows that rutin has formed nine hydrophobic interactions and six hydrogen bonds.

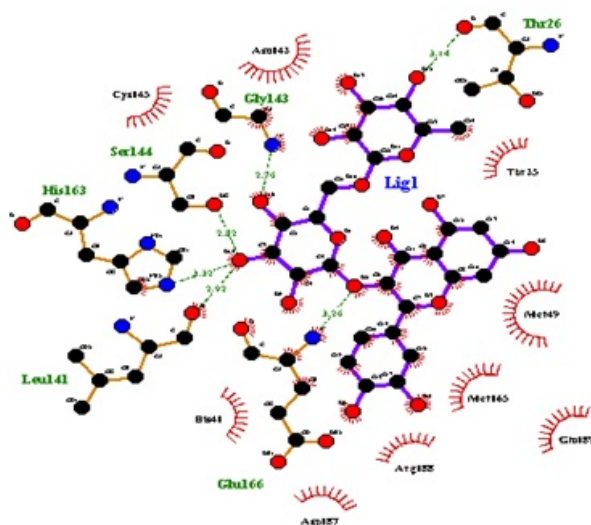


FIGURE 4.11: Interaction of rutin with receptor protein

Figure 4.12 shows the interaction of apigenin with receptor protein M^{pro} . It shows that apigenin has formed nine hydrophobic interactions and four hydrogen bonds.

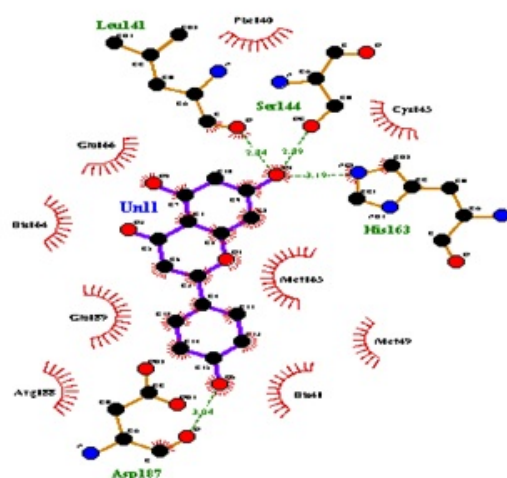


FIGURE 4.12: Interaction of apigenin with receptor protein

Figure 4.13 shows the interaction of chrysoplenetin with receptor protein M^{pro} . It shows that chrysoplenetin has formed nine hydrophobic interactions and seven hydrogen bonds.

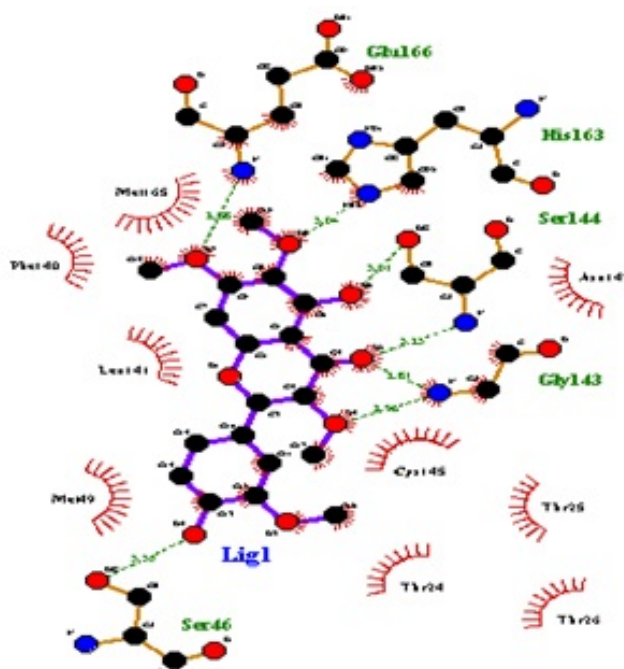


FIGURE 4.13: Interaction of chrysoplenetin with receptor protein

Figure 4.14 shows the interaction of arteannunin b with receptor protein M^{pro} . It shows that arteannunin b has formed six hydrophobic interactions and two hydrogen bonds.

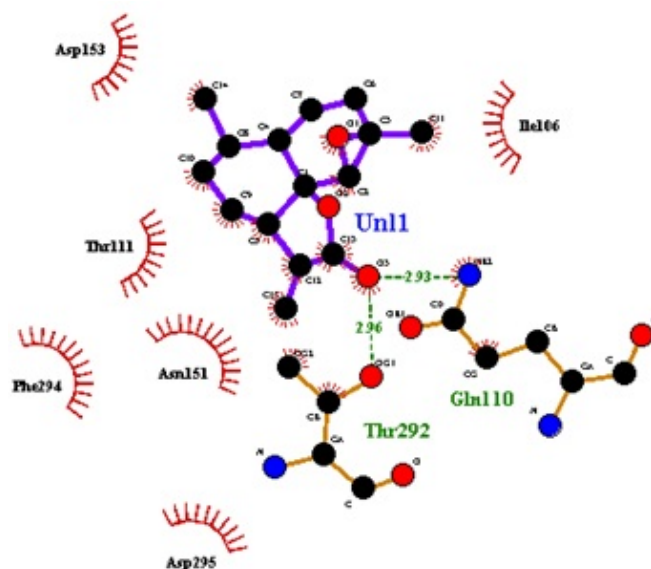


FIGURE 4.14: Interaction of arteannunin b with receptor protein

Figure 4.15 shows the interaction of artemisinin with receptor protein M^{pro} . It shows that artemisinin has formed seven hydrophobic interactions and one hydrogen bond.

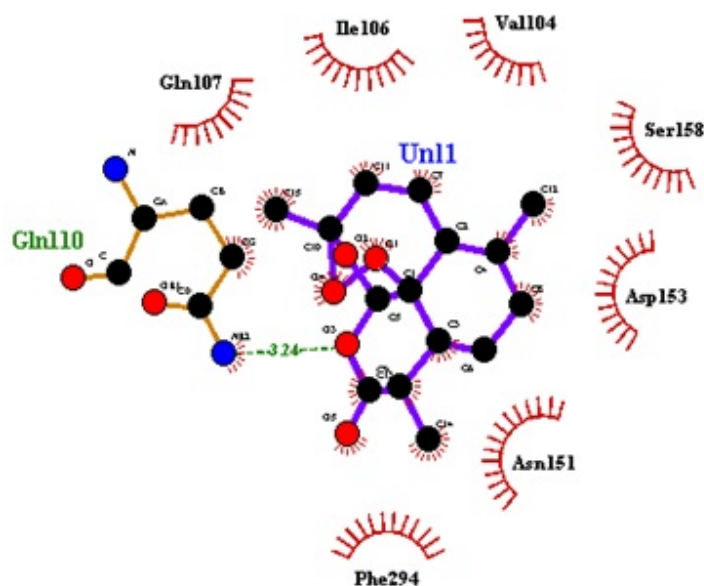


FIGURE 4.15: Interaction of artemisinin with receptor protein

Figure 4.16 shows the interaction of scopoletin at the 3rd cavity with receptor protein M^{pro} . It shows that scopoletin has formed three hydrophobic interactions and six hydrogen bonds.

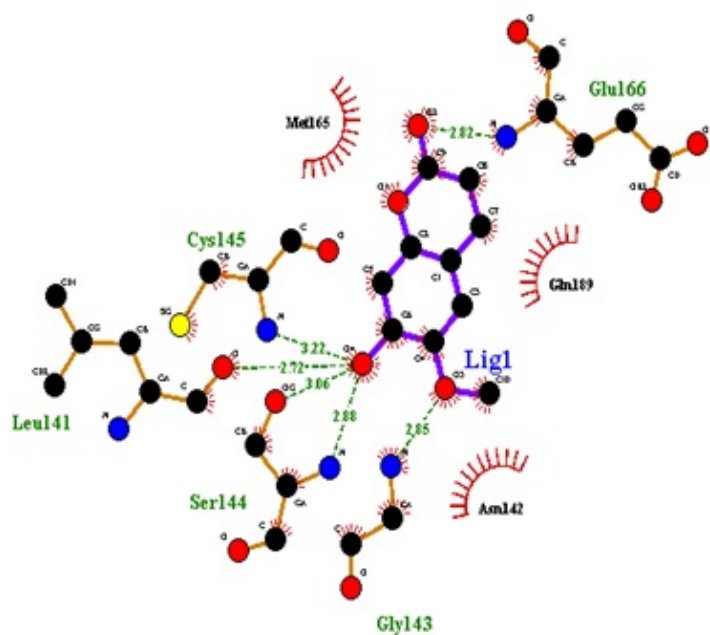


FIGURE 4.16: Interaction of scopoletin at 3rd cavity with receptor protein

Figure 4.17 shows the interaction of scopoletin at cavity 5th with receptor protein M^{pro} . It shows that scopoletin has formed six hydrophobic interactions and two hydrogen bonds.

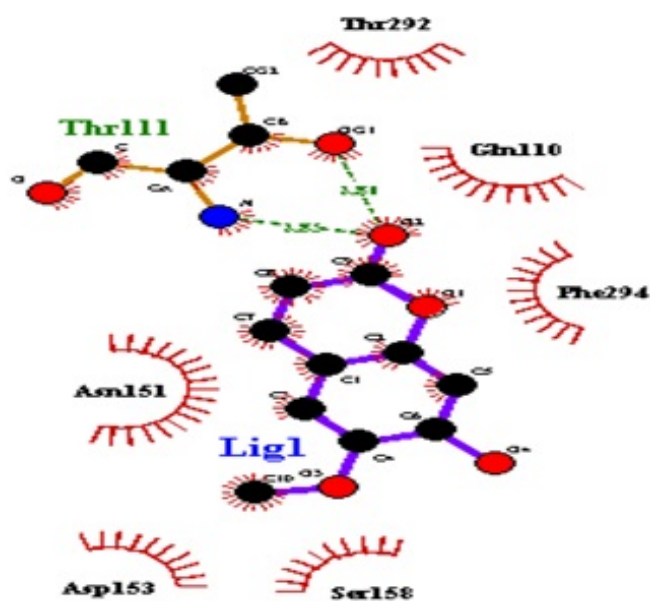


FIGURE 4.17: Interaction of scopoletin at 5th cavity with receptor protein

Figure 4.18 shows the interaction of scoparone with receptor protein M^{pro} . It shows that scoparone has formed eight hydrophobic interactions and two hydrogen bonds.

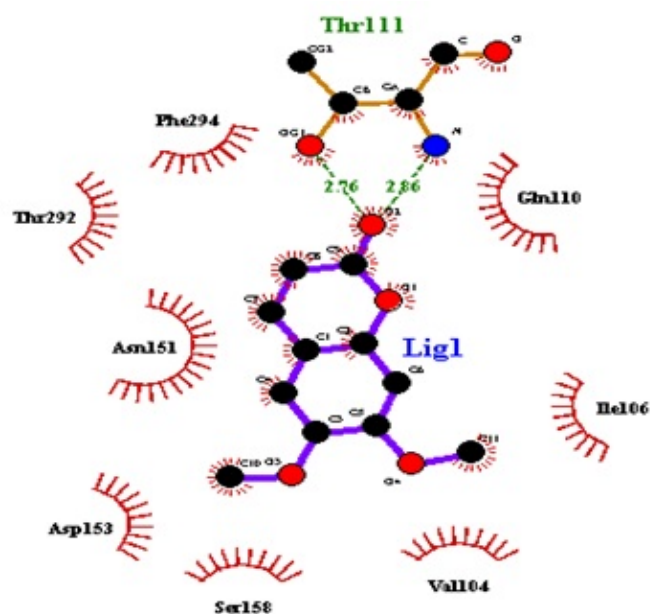


FIGURE 4.18: Interaction of scoparone with receptor protein

Figure 4.19 shows the interaction of artemisic acid with receptor protein M^{pro} . It shows that Artemisic acid has formed four hydrophobic interactions and four hydrogen bonds.

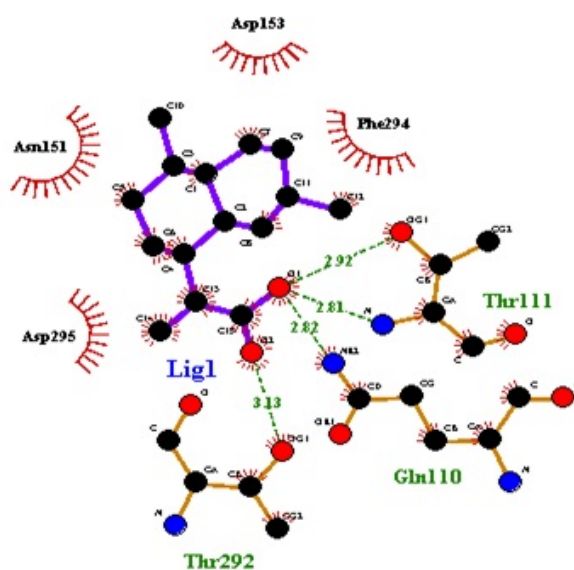


FIGURE 4.19: Interaction of artemisic acid with receptor protein

Figure 4.20 shows the interaction of deoxyartemisinin with receptor protein M^{pro} . It shows that deoxy artemisinin has formed eight hydrophobic interactions and two hydrogen bonds.

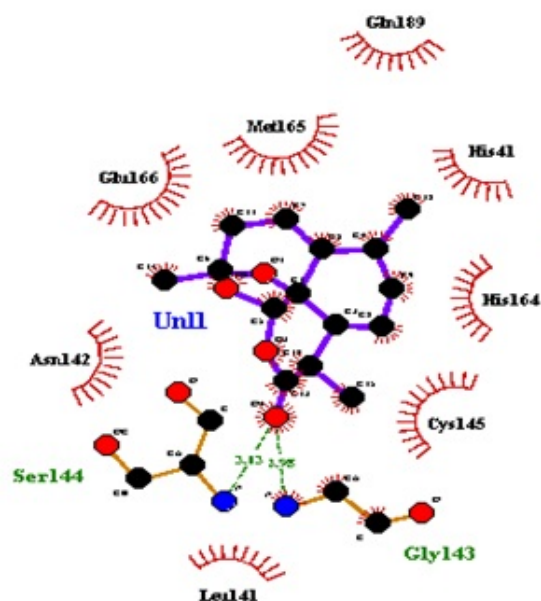


FIGURE 4.20: Interaction of deoxyartemisinin with receptor protein

Figure 4.21 shows the interaction of artemetin with receptor protein M^{pro}. It shows that artemetin has formed eight hydrophobic interactions and seven hydrogen bonds.

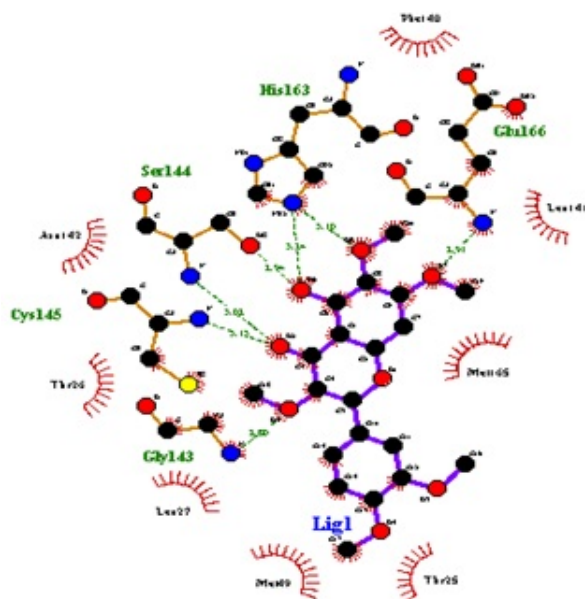


FIGURE 4.21: Interaction of artemetin with receptor protein

Figure 4.22 shows the interaction of casticin with receptor protein M^{pro}. It shows that casticin has formed ten hydrophobic interactions and seven hydrogen bonds.

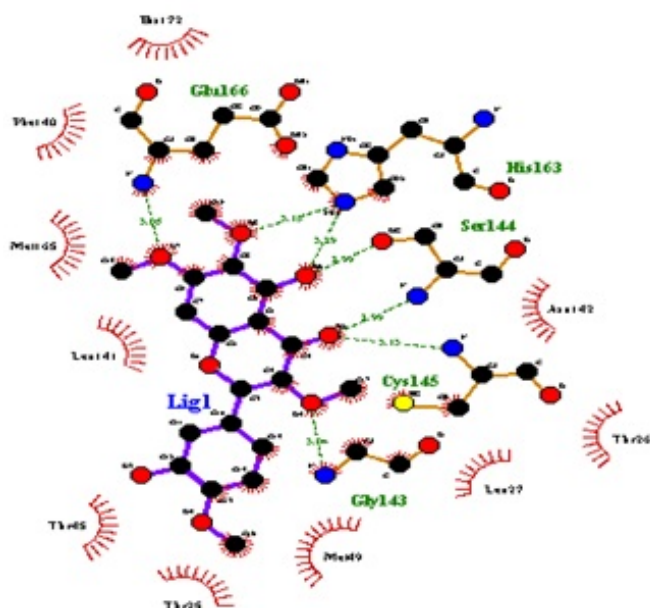


FIGURE 4.22: Interaction of casticin with receptor protein

Figure 4.23 shows the interaction of sitogluside at 1st cavity with receptor protein M^{pro} . It shows that sitogluside has formed eight hydrophobic interactions and five hydrogen bonds.

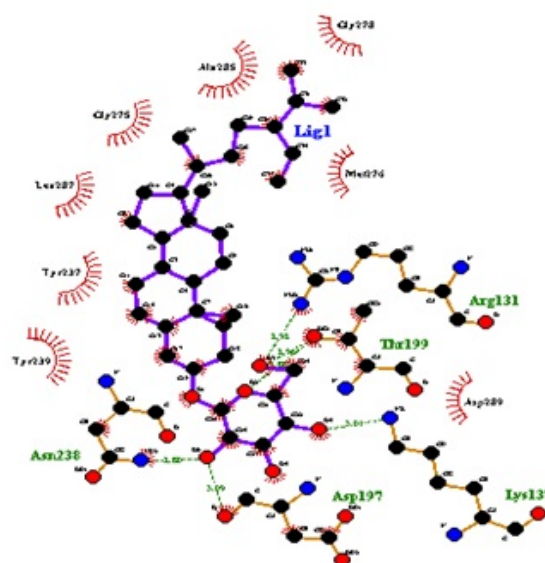


FIGURE 4.23: Interaction of sitogluside at cavity 1 with receptor protein

Figure 4.24 shows the interaction of sitogluside at the 4th cavity with receptor protein M^{pro} . It shows that sitogluside has formed nine hydrophobic interactions and two hydrogen bonds.

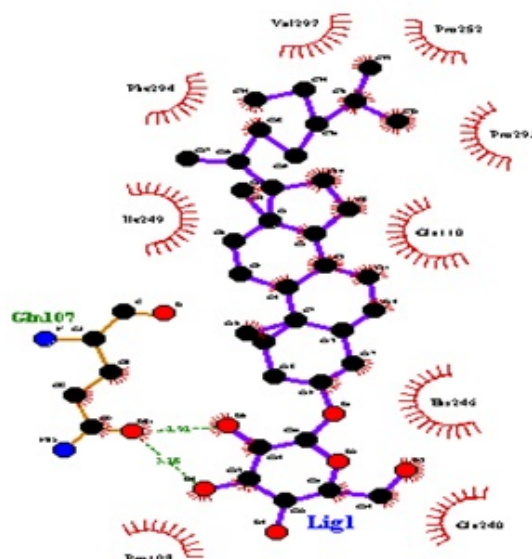


FIGURE 4.24: Interaction of sitoglucoside at cavity 4 with receptor protein

Figure 4.25 shows the interaction of beta-sitosterol with receptor protein M^{pro} . It shows that beta-sitosterol has formed nine hydrophobic interactions and one hydrogen bond.

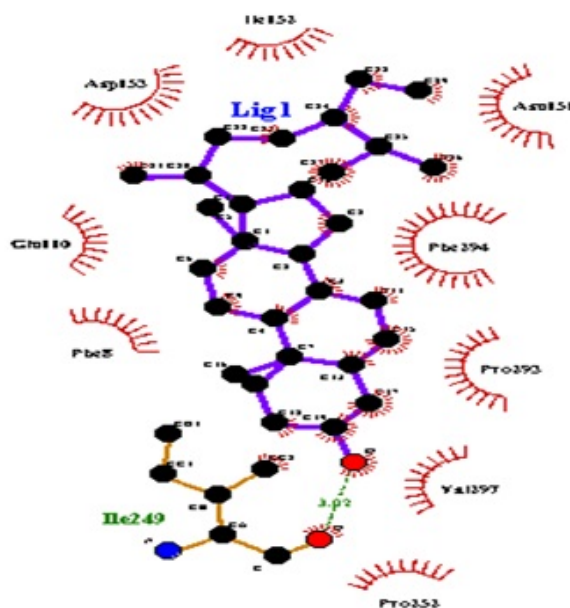


FIGURE 4.25: Interaction of beta-sitosterol with receptor protein

Figure 4.26 shows the interaction of dihydroartemisinin with receptor protein M^{pro} . It shows that dihydroartemisinin has formed seven hydrophobic interactions and one hydrogen bond.

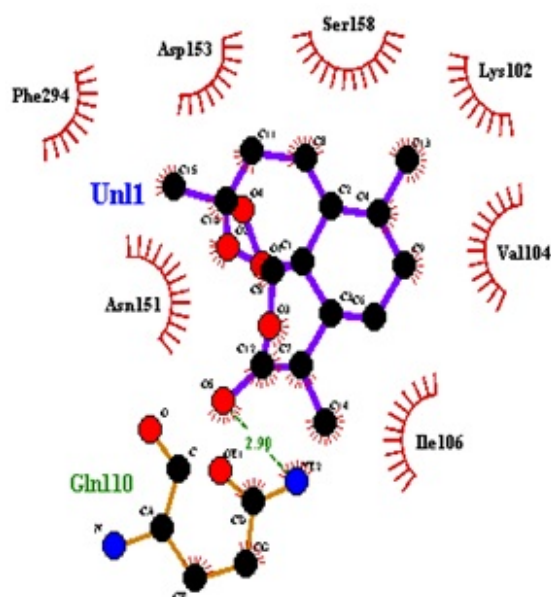


FIGURE 4.26: Interaction of dihydroartemisinin with receptor protein

Figure 4.27 shows the interaction of scopolin with receptor protein M^{pro} . It shows that scopolin has formed eight hydrophobic interactions and eight hydrogen bonds.

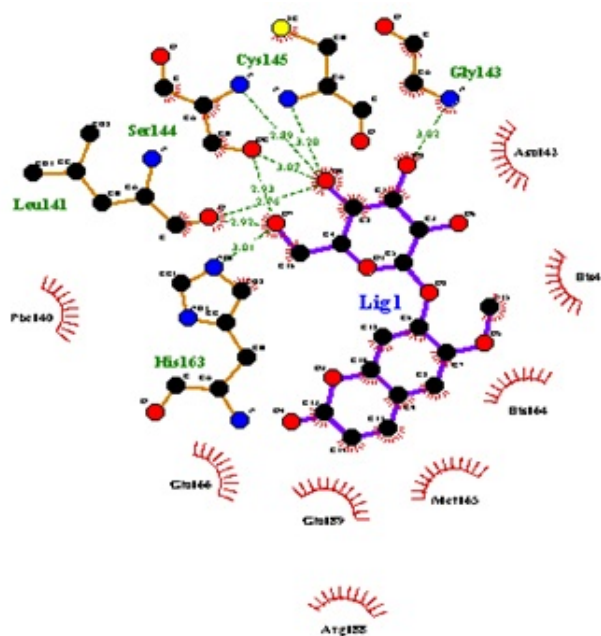


FIGURE 4.27: Interaction of scopolin with receptor protein

Figure 4.28 shows the interaction of artemether with receptor protein M^{pro} . It shows that artemether has formed six hydrophobic interactions and two hydrogen bonds.

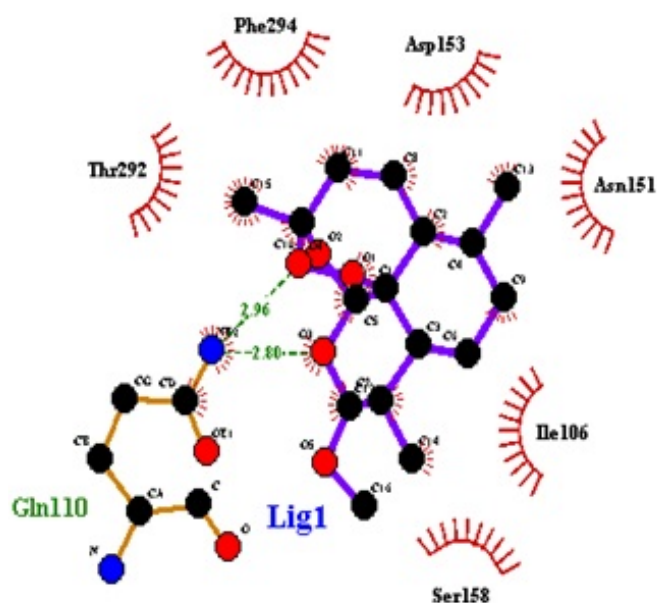


FIGURE 4.28: Interaction of artemether with receptor protein

Figure 4.29 shows the interaction of artemotil with receptor protein M^{pro} . It shows that artemotil has formed thirteen hydrophobic interactions.

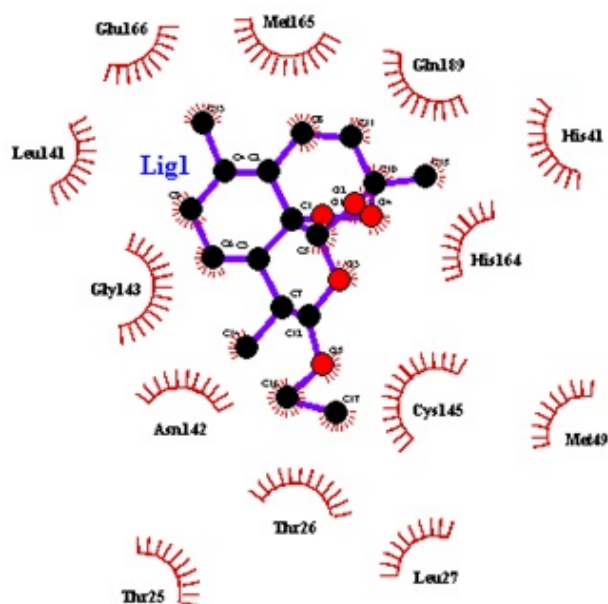


FIGURE 4.29: Interaction of artemotil with receptor protein

Figure 4.30 shows the interaction of artesunate with receptor protein M^{pro} . It shows that artesunate has formed nine hydrophobic interactions and three hydrogen bonds.

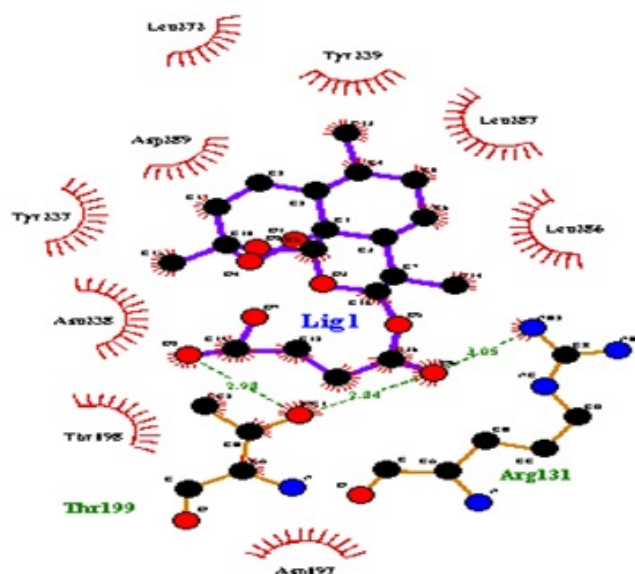


FIGURE 4.30: Interaction of artesunate with receptor protein

The Table 4.6 below shows the details of hydrogen and hydrophobic interactions of the selected ligands with the receptor protein. The values show that artemotil forms the highest hydrophobic interactions in number which is thirteen next is casticin with 10 hydrophobic bonds, nine hydrophobic bonds are made by artesunate, beta-sitosterol, sitogluside at cavity 4, rutin, apigenin, quercetin, and chrysopenetin with that 8 hydrophobic interactions are made by scoparone, deoxy artemisinin, artemetin, sitogluside at cavity 1 and scopolin.

The hydrogen bonds formed by quinic acid are 10 which is the highest in number out of all the selected ligands whereas scopolin forms eight hydrogen bonds. Casticin, artemetin and chrysopenetin forms seven hydrogen bonds

TABLE 4.6: Active ligand showing hydrogen and hydrophobic interactions

S. No.	Ligand Name	Binding Energy	No. of HBs	Hydrogen Bonding		Hydrophobic Bonding
				Amino Acids	Distance	
1	α -pinene	-4.8	0	-	-	Thr111 Gln110

						Phe8
						Asn151
						Ile152
						Phe294
2	β pinene	-4.7	0	-	-	Ser158
						Asn151
						Phe294
						Asp153
3	Carvone	-5.1	1	NE2-Gln 110-O	3.1	Ile106
						Asn151
						Asp153
						Phe294
						Ile152
						Phe8
4	Myrtenol	-5.2	3	OG1-Thr 111-O	2.85	Gln110
				N-Thr111-O	2.89	Asn151
				O-Thr111-O	3.14	Thr292
						Phe294
5	Quinic acid	-5.4	10	N-Glu166-O2	2.99	Phe140
				N-Gly143-O5	3.33	Met165
				N-Gly143-O6	3.1	Asn142
				N-Cys145-O6	3.25	
				N-Ser144-O6	2.87	
				OG-Ser144-O6	3.11	
				OG-Ser144-O4	3.03	
				O-Leu141-O6	2.72	
				O-Leu141-O4	2.99	

				NE2-His	3.02	
				163-O4		
6	Caffeic acid	-6	5	OG1-Thr	2.88	Asp295
				292-O4		
				NE2-Gln	2.95	Phe294
				110-O3		
				N-Thr111-O3	2.87	Asn151
				OG-Ser	3.26	Asp153
				158-O1		
				OG-Ser	2.84	Val104
				158-O2		
7	Quercetin	-7.6	2	O-Thr190-O4	3.03	Arg188
				O-Asp187-O7	3.07	His41
						His164
						Met165
						Glu166
						Leu167
						Pro168
						Gln192
						Gln189
8	Rutin	-8.9	6	N-Glu166-O2	3.26	Thr25
				O-Leu141-O15	2.92	Met49
				NE2-His	3.32	Gln189
				163-O15		
				OG-Ser	2.82	Met165
				144-O15		
				N-Gly	2.76	Arg188
				143-O16		
				O-Thr26-O12	3.14	Asp187
						His41
						Cys145
						Asn142

9	Apigenin	-7.8	4	O-Leu141-O4	2.84	Phe140
				OG-Ser 144-O4	2.89	Cys145
				NE2-His 163-O4	3.19	Met49
				O-Asp187-O5	3.04	Met165
						His41 Arg188 Gln189 His164 Glu166
10	Chryso- plenetin	-7.7	7	OG-Ser46-O4	3.35	Asn142
				N-Gly143-O5	2.96	Cys145
				N-Gly143-O2	2.81	Thr25
				N-Ser144-O2	3.23	Thr24
				OG-Ser 144-O6	3.01	Thr26
				NE2-His 163-O8	3.04	Met49
				N-Glu166-O7	2.88	Leu141 Phe140 Met165
11	Artean- ninin b	-6.6	2	NE2-Gln 110-O3	2.93	Ile106
				OG1-Thr 292-O3	2.96	Asp295
						Asn151 Phe294 Thr111 Asp153

12	Artemisinin	-7	1	NE2-Gln	3.24	Gln107
				110-O3		Ile106
						Val104
						Ser158
						Asp153
						Asn151
						Phe294
13	Scopoletin	-8.9	6	N-Glu166-O2	2.82	Met165
				N-Cys145-O4	3.22	Gln189
				O-Leu141-O4	2.72	Asn142
				OG-Ser144-O4	3.06	
				N-Ser144-O4	2.88	
				N-Gly143-O3	2.85	
		-10.9	2	N-Thr111-O2	2.85	Thr292
				OG1-Thr	2.81	Gln110
				111-O2		Phe294
						Ser158
14	Scoparone	-6	2	N-Thr111-O2	2.86	Gln110
				OG1-Thr	2.76	Ile106
				111-O2		Val104
					Ser158	
					Asp153	
	Asn151					
	Thr292					
	Phe294					

15	Artemisnic acid	-7	4	OG1-Thr	2.92	Asp153		
				111-O1				
				N-Thr111-O1			2.81	Phe294
				NE2-Gln			2.82	Asp295
110-O1								
16	Deoxy-artemisinin	-7.2	2	OG1-The	3.13	Asn151		
				292-O2				
				N-Ser144-O4			3.13	Asn142
				N-Gly143-O4			2.98	Glu166
						Met165		
						Gln189		
						His41		
						His164		
						Cys145		
						Leu141		
17	Artemetin	-7.6	7	N-Glu166-O7	2.91	Phe140		
				N-Gly143-O5	2.8	Leu141		
				N-Cys145-O2	3.13	Met165		
				N-Ser144-O2	3.02	Thr25		
				OG-Ser	2.94	Met49		
				144-O6				
				NE2-His	3.24	Leu27		
163-O6								
NE2-His	3.1	Thr26						
163-O8								
						Asn142		
18	Casticin	-7.6	7	N-Gly143-O5	3.04	Asn142		
				N-Cys145-O2	3.13	Thr26		
				N-Ser144-O2	2.99	Leu27		

				OG-Ser	2.99	Met49
				144-O6		
				NE2-His	3.29	Thr25
				163-O6		
				NE2-His	3.15	Thr45
				163-O8		
				N-Glu166-O7	3.05	Leu141
						Met165
						Phe140
						His172
19	Sitog- luside	-8.6	5	NH2-Arg	2.92	Tyr239
				131-O3		
				OG1-Thr	2.96	Tyr237
				199-O3		
				NZ-Lys	3.01	Leu287
				137-O4		
				O-Asp197-O6	3.09	Gly275
				ND2-Asn	2.8	Ala285
				238-O6		
						Gly278
						Met276
						Asp289
		-11.6	2	OE1-Gln	2.92	Ile249
				107-O6		
				OE1-Gln	3.28	Phe294
				107-O5		
						Val297
						Pro252
						Pro293
						Gln110
						His246
						Glu240

						Pro108
20	Beta-sitosterol	-6.9	1	O-Ile249-O	3.02	Phe8
						Gln110
						Asp153
						Ile152
						Asn151
						Phe294
						Pro293
						Val297
						Pro252
21	Dihydro-artemisinin	-7.1	1	NE2-Gln 110-O5	2.9	Asn151
						Phe294
						Asp153
						Ser158
						Lys102
						Val104
						Ile106
22	Scopolin	-7.5	8	NE2-His 163-O7	3.01	Asn142
				O-Leu141-O7	2.92	His41
				O-Leu141-O9	2.76	His164
				OG-Ser144-O7	2.93	Met165
				OG-Ser144-O9	3.07	Gln189
				N-Ser144-O9	2.89	Arg188
				N-Cys145-O9	3.2	Glu166
				N-Gly143-O8	3.02	Phe140
23	Artemether	-7.1	2	NE2-Gln 110-O4	2.96	Asp153

4.6 ADME Properties of Ligand

Lipinski's rule of five (molecular weight ≤ 500 , HBA ≤ 10 , HBD ≤ 5 and logP value ≤ 5) is used as a first step for the assessment of availability either verbal or artificial [57]. pkCSM is the second tool that is used for the assessment of ADME properties [56].

4.6.1 Pharmacodynamics

One of the broader terms used in pharmacology is pharmacodynamics which deals with the study of drug effects on the body [65].

4.6.2 Pharmacokinetics

The other term used in pharmacology is pharmacokinetics which deals with the study of the effect of the body on the drug, that how the body reacts after the drug enters the body. The absorption, distribution, metabolism, and excretion of drugs are also studied [65].

4.6.3 Absorption

The CaCO₂ solubility helps in predicting the absorption of the drugs which are administered orally. Value >0.90 (log Papp in 10⁻⁶ cm/s) is considered as high CaCO₂ permeability [63-65, 67]. The water solubility of the ligands is given as log mol/L. this indicates the compound solubility in water at 25°C. hence the lipid-soluble drugs will be less soluble than the water-soluble drugs [64, 65, 67, 68]. Intestinal absorption indicates the value or proportion of the compound that will absorb into the intestines. A value less than 30% is considered poorly absorbed [64, 65, 67, 68]. P-glycoprotein is an ABC transporter that functions to extrude toxins or other xenobiotics from the cells by acting as a biological barrier [64, 65, 67, 68].

P-glycoprotein inhibition can be a therapeutic target or it can act in contradiction [64, 65, 67, 68]. Skin permeability is important for developing transdermal drugs. Any compound with a value > -2.5 has a low skin permeability [64, 65, 67, 68]. The absorption properties of selected ligands and azithromycin are given in Table 4.7.

TABLE 4.7: Absorption properties of selected ligands and standard drug

Ligands	Water Solubility Log mol/L	Ca CO ₂ Solubility log P	Intestinal Absorption	Skin Permeability	P-glycoprotein substrate	P-glycoprotein I inhibitor	P-glycoprotein II inhibitor
α -pinene	-3.733	1.38	96.041	-1.827	No	No	No
β -pinene	-4.191	1.385	95.525	-1.653	No	No	No
Carvone	-2.324	1.413	97.702	-2.145	No	No	No
Myrtenol	-2.384	1.464	94.34	-2.347	No	No	No
Quinic acid	-1.119	-0.258	32.274	-2.737	No	No	No
Caffeic acid	-2.33	0.634	69.407	-2.722	No	No	No
Quercetin	-2.925	-0.229	77.207	-2.735	Yes	No	No
Rutin	-2.892	-0.949	23.446	-2.735	Yes	No	No
Casticin	-3.599	1.39	96.91	-2.744	Yes	No	Yes
Chryso-plenetin	-3.605	1.393	99.856	-2.743	Yes	No	Yes
Apigenin	-3.329	1.007	93.25	-2.735	Yes	No	No
Arteann-unin b	-3.221	1.537	98.347	-3.322	No	No	No
Artemis-inic acid	-3.632	1.6	95.706	-2.699	No	No	No
Artem-isinin	-3.678	1.295	97.543	-3.158	No	No	No

Deoxyar-temisinin	-3.396	1.318	97.828	-3.279	No	No	No
Dihydroar-temisinin	-3.699	1.249	94.965	-3.354	No	No	No
Artemetin	-4.326	1.424	100	-2.747	Yes	Yes	Yes
Artemether	-3.927	1.311	96.855	-2.929	No	Yes	No
Artemotil	-3.908	1.332	96.488	-3.345	No	Yes	No
Artesunate	-3.097	0.863	72.19	-2.735	Yes	No	No
Scopoletin	-2.504	1.184	95.277	-2.944	No	No	No
Scoparone	-1.976	1.298	97.879	-2.346	No	No	No
Scopolin	-2.21	0.377	48.119	-2.822	Yes	No	No
Sitogluside	-4.741	0.472	79.677	-2.748	Yes	Yes	Yes
Beta-sitosterol	-6.773	1.201	94.464	-2.783	No	Yes	Yes
Azithromycin	-4.133	-0.211	45.808	-2.742	Yes	Yes	No

The water solubility of each compound shows solubility at 25°C. The results of absorption show that quinic acid, caffeic acid, quercetin, rutin, sitogluside, scopolin and artesunate have low CaCO₂ solubility. Out of all the ligands only rutin shows the poor intestinal absorption.

The skin permeability results predict that all the ligands are skin permeable. As for P-glycoprotein substrates quercetin, scopolin, rutin, artesunate, apigenin, sitogluside, chrysoplenetin, artemetin and casticin acts as P-glycoprotein substrates. Artemetin, sitogluside, beta-sitosterol, artemether and artemotil acts as P-glycoprotein I inhibitors whereas, all other ligands are not the inhibitors. Artemetin, sitogluside, beta-sitosterol along with casticin and chrysoplenetin acts as P-glycoprotein II inhibitors.

The values show that azithromycin shows a very low CaCO₂ solubility and water solubility. Though the intestinal absorption is low but it still is in the safe range. Azithromycin also has a lower value of skin permeability. Azithromycin

is also a P-glycoprotein substrate and an inhibitor to P-glycoprotein I but not a P-glycoprotein II inhibitor.

Some of the parameters of absorption properties of α -pinene has already been studied by P Bhattacharya, TN Patel – 2021 [63]. Some parameters of absorption properties of β -pinene and carvone have been studied by Erman Salih İSTİFLİ in 2020 [64]. Pkcs_m absorption properties of myrtenol, arteannunin b, deoxyartemisinin, artemetin, casticin, scopolin, artemether, artesunate, artemisinin, scopoletin, scoparone and artemisnic acid have already been reported by Zarina Khurshid in 2021 [65].

Some parameters of absorption of quercetin, rutin and apigenin have been studied by Oluwaseun Taofeek in 2020 [67]. Absorption properties of beta sitosterol has already been reported by Muthumanickam Sankar and his colleagues in 2021 [68].

4.6.4 Distribution

The VD_{ss} is the theoretical volume which tells about the total dose of the drug which will be needed to be distributed uniformly to give the same concentration as it is in the blood plasma. If the VD_{ss} value exceeds 2.81 L/kg, then the drug is more distributed in the tissues than in the plasma. The VD_{ss} will be low if the value is below 0.71 L/kg [65].

Many drugs in the plasma exist in an equilibrium between a bounded and an unbounded state to the serum proteins. As a drug binds more to the serum proteins it will have less efficiency of diffusion to cellular membranes.

The blood-brain barrier protects the brain and reduces the exogenous compounds to enter directly into the brain. If a compound has a value of logBB >0.3 then it will easily cross the BBB barrier hence been effective and if it is logBB <-1 then it is poorly distributed [65].

Compounds with a value of logPS >-2 penetrate the CNS whereas value logPS ≤ -3 does not penetrate the CNS [65].

TABLE 4.8: Distribution of selected ligands and standard drug.

S. No	Ligand	VD _{ss} (human) L/Kg	Fraction unbound (human)	BBB Perme- ability logBB	CNS Perme- ability logPS
1.	Alpha-pinene	0.667	0.425	0.791	-2.201
2.	Beta pinene	0.685	0.35	0.818	-1.857
3.	Carvone	0.179	0.53	0.588	-2.478
4.	Myrtenol	0.488	0.499	0.773	-2.511
5.	Quinic acid	-0.271	0.821	-0.894	-3.667
6.	Caffeic acid	-1.098	0.529	-0.647	-2.608
7.	Quercetin	-1.559	0.20	-1.098	-3.065
8.	Rutin	1.663	0.187	-1.899	-5.178
9.	Apigenin	0.822	0.147	-0.734	-2.061
10.	Chrysoplenetin	-0.161	0.103	-1.043	-3.226
11.	Arteannunin b	0.401	0.426	0.434	-2.951
12.	Artemisinin	0.457	0.4	0.235	-2.909
13.	Scopoletin	0.034	0.363	-0.299	-2.32
14.	Scoparone	-0.344	0.298	0.177	-2.328
15.	Artemisnic acid	-0.449	0.302	0.323	-2.314
16.	Deoxyartemisnin	0.356	0.411	0.28	-2.999
17.	Artemetin	-0.244	0.123	-1.152	-3.156
18.	Casticin	-0.176	0.103	-1.053	-3.209
19.	Sitogluside	-1.163	0.078	-0.785	-3.021
20.	Beta-sitosterol	0.193	0	0.781	-1.705
21.	Dihydroartemisnin	0.613	0.452	0.783	-2.952
22.	Scopolin	-0.611	0.397	-1.286	-3.954
23.	Artemether	0.611	0.384	0.861	-3.239
24.	Artemotil	0.448	0.376	0.253	-3.359
25.	Artesunate	0.172	0.36	-0.954	-3.039

26.	Azithromycin	-0.214	0.512	-1.857	-3.777
-----	--------------	--------	-------	--------	--------

The parameters through which the distribution properties are determined includes VDss which is in the given range to be distributed in the blood and the tissues. The values of the fraction unbound of these ligands shows that out of the total dose this fraction will not be bounded to the protein. α -pinene, β -pinene, carvone, myrtenol and quinic acid can cross the blood brain barriers whereas quinic acid will not pass the CNS.

Some of the parameters of distribution properties of α -pinene has already been studied by P Bhattacharya, TN Patel – 2021 [63]. Some parameters of distribution properties of β -pinene and carvone have been studied by Erman Salih Istifli in 2020 [64]. PkcsM distribution properties of myrtenol has already been reported by Zarina Khurshid in 2021 [65].

The table indicates that quercetin and rutin cannot cross the blood brain barrier and with that quercetin, rutin and chrysoplenetin are not permeable to central nervous system. Some parameters of distribution of quercetin, rutin and apigenin have been studied by Oluwaseun Taofeek in 2020 [67]. The values mentioned in the table indicates that arteannunin b, artemisnin, scopoletin, scoparone and artemisnic acid are permeable to the central nervous system and that they can easily cross the blood brain barrier. PkcsM Distribution properties of Arteannunin b, Artemisnin, Scopoletin, Scoparone and Artemisnic acid have already been reported by Zarina Khurshid in 2021 [65].

Artemetin, casticin and sitogluside all three ligands can not pass through the central nervous system. Casticin can poorly pass the blood brain barrier. PkcsM distribution properties of deoxyartemisnin, artemetin and casticin have already been reported by Zarina Khurshid in 2021 [65]. Distribution properties of beta sitosterol has already been reported by Muthumanickam Sankar and his colleagues in 2021 [68].

The table indicates that scopolin will poorly pass the blood-brain barrier. It also shows that scopolin, artemether, artemotil and artesuante cannot pass through

the central Pk_{sm} Distribution properties of scopolin, artemether and artesunate have already been reported by Zarina Khurshid in 2021 [65].

The distribution parameters value of azithromycin shows that the value of VD_{ss} is low which means the drug would not be distributed properly. Azithromycin can penetrate in CNS and also can pass the blood brain barrier

4.6.5 Metabolism

Cytochrome P450 is an enzyme held responsible for detoxification in the liver. Many drugs get deactivated by this enzyme but certain drugs can be activated. Inhibitors of this enzyme can directly affect the metabolism of drug hence should not be used [65-68]. Similarly, CYP2D6 and CYP3A4 are responsible for the metabolism of the drugs. Inhibition to these affects the pharmacokinetics of the drug in use [65-68]. Table 4.9 shows that all the ligands are not CYP2D6 substrates, only chrysoplenetin, arteannunin b, artemisinin, deoxyartemisinin, artemetin, casticin, sitogluside, beta-sitosterol, artesunate, artemether and artemotil are all CYP3A4 substrates. Quercetin, apigenin, chrysoplenetin, arteannunin b, artemisinin, scopoletin, scoparone, deoxyartemisinin, artemetin, casticin and artemether are all artem- ether are all CYP1A2 inhibitors.

TABLE 4.9: Metabolic properties of selected ligands and standard drug

S. No.	Ligands	CYP-2D6 subst- rate	CYP-3A4 subst- rate	CYP-1A2 inhi- bitor	CYP-2C19 inhi- bitor	CYP-2C9 inhi- bitor	CYP-2D6 inhi- bitor	CYP-3A4 inhi- bitor
1	α -pinene	No	No	No	No	No	No	No
2	β -pinene	No	No	No	No	No	No	No
3	Carvone	No	No	No	No	No	No	No
4	Myrtenol	No	No	No	No	No	No	No
5	Quinic acid	No	No	No	No	No	No	No

6	Caffeic acid	No	No	No	No	No	No	No
7	Quercetin	No	No	Yes	No	No	No	No
8	Rutin	No	No	No	No	No	No	No
9	Casticin	No	Yes	Yes	Yes	No	No	Yes
10	Chryso- plenetin	No	Yes	Yes	Yes	No	No	Yes
11	Apigenin	No	No	Yes	Yes	No	No	No
12	Artean- ninin b	No	Yes	Yes	No	No	No	No
13	Artemis- inic acid	No	No	No	No	No	No	No
14	Artem- isinin	No	Yes	Yes	No	No	No	No
15	Deoxyar- temisinin	No	Yes	Yes	No	No	No	No
16	Dihydro- artemisinin	No	No	No	No	No	No	No
17	Artemetin	No	Yes	Yes	Yes	Yes	No	No
18	Artemether	No	Yes	Yes	No	No	No	No
19	Artemotil	No	Yes	No	No	No	No	No
20	Artesunate	No	Yes	No	No	No	No	No
21	Scopoletin	No	No	Yes	No	No	No	No
22	Scoparone	No	No	Yes	No	No	No	No
23	Scopolin	No	No	No	No	No	No	No
24	Sitogluside	No	Yes	No	No	No	No	No
25	Beta-sito- sterol	No	Yes	No	No	No	No	No
26	Azithro- mycin	No	Yes	No	No	No	No	No

Apigenin, chrysoplenetin, artemetin and casticin are CYP2C19 inhibitor. Only artemetin is a CYP2C9 inhibitor. All the ligands are not CYP2D6 inhibitor. Chrysoplenetin and casticin are CYP3A4 inhibitor.

The table indicates that azithromycin is not a CYP2D6 substrate rather than it is a CYP3A4 substrate. Azithromycin is not a CYP1A2, CYP2C19, CYP2C9, CYP2D6 and CYP3A4 inhibitor.

Some of the parameters of metabolic properties of alpha-pinene has already been studied by P Bhattacharya, TN Patel – 2021 [63]. Some parameters of metabolic properties of beta-pinene and carvone have been studied by Erman Salih Istifli in 2020 [64].

Pksm metabolic properties of myrtenol, arteannunin b, artemisnin, scopoletin, scopolin, artemether, artesunate, scoparone, deoxyartemisnin, artemetin, casticin and artemisnic acid have already been reported by Zarina Khurshid in 2021 [65].

Some parameters of metabolism of quercetin, rutin and apigenin have been studied by Oluwaseun Taofeek in 2020 [67]. Metabolic properties of beta sitosterol has already been reported by Muthumanickam Sankar and his colleagues in 2021 [68].

4.6.6 Excretion

The Renal OCT2 substrate acts as a transporter that helps in clearing the drugs and other compounds. Total clearance indicates hepatic clearance which means the drug is metabolized and renal clearance indicates the drug is excreted [65-68]. The excretion values of the ligands are given below.

Table 4.10 shows the Excretory Properties of alpha-pinene, beta-pinene, carvone, myrtenol, and quinic acid. The table indicates that all these ligands are not renal OCT2 substrates which means the ligands would not be cleared out of the body and hence the total clearance values are given accordingly.

TABLE 4.10: Excretion of selected ligands and standard drug

S. No.	Ligands	Total Clearance	Renal OCT2 Substrate
1	α -pinene	0.043	No
2	β -pinene	0.03	No
3	Carvone	0.225	No
4	Myrtenol	0.054	No
5	Quinic acid	0.630	No
6	Caffeic acid	0.508	No
7	Quercetin	0.407	No
8	Rutin	-0.369	No
9	Casticin	0.628	No
10	Chrysoplenetin	0.627	No
11	Apigenin	0.566	No
12	Arteannunin b	0.965	No
13	Artemisinic acid	0.639	No
14	Artemisinin	0.98	No
15	Deoxyartemisinin	0.803	No
16	Dihydroartemisinin	1.002	No
17	Artemetin	0.706	No
18	Artemether	1.031	No
19	Artemotil	1.068	No
20	Artesunate	0.969	No
21	Scopoletin	0.73	No
22	Scoparone	0.793	No
23	Scopolin	0.716	No
24	Sitogluside	0.689	No
25	Beta-sitosterol	0.628	No
26	Azithromycin (Standard Drug)	-0.424	No

The table indicates that all these ligands and standard drug are not renal OCT2 substrates which means they would not be cleared out of the body and hence the total clearance values are given accordingly. Some of the parameters of excretory properties of alpha-pinene has already been studied by P Bhattacharya, TN Patel – 2021 [63]. Some parameters of excretory properties of beta-pinene and carvone have been studied by Erman Salih Istifli in 2020 [64]. Pk_{cs}m excretory properties of myrtenol , arteannunin b, artemisinin, scopoletin, scoparone, artemisnic acid, deoxyartemisinin, artemetin, scopolin, artemether, artesunate and casticin have already been reported by Zarina Khurshid in 2021 [65]. Some parameters of excretion properties of quercetin, rutin and apigenin have been studied by Oluwaseun Taofeek in 2020 [67]. Excretion properties of beta sitosterol has already been reported by Muthumanickam Sankar and his colleagues in 2021 [61].

4.7 Lead Compound Identification

The physiochemical and the pharmacokinetics properties of the ligands determine their fate as for being drug or non-drug compounds. Lipinski's rule is the first filter and pharmacokinetics is the second filter for this identification. Rutin does not follow the Lipinski Rule as the Molecular weight, H bond acceptors, and hydrogen bond donor values of Rutin exceed the Lipinski rule, with that Log P-value and Molecular weight value of Sitogluside does not abides by the rule but as it falls from two it is acceptable. The Log P value of Beta-sitosterol is also more than 5 but it is still passed to the next stage. So, in the first stage, only Rutin has been knocked out. The next knockout stage is pharmacokinetic screening. In this screening Artemisinin and Dihydroartemisinin because of being carcinogenic have been knocked out. Beta-sitosterol being an hERG II inhibitor has also been knocked out. At the end of this, the compounds left are alpha-pinene, beta-pinene, myrtenol, quinic acid, caffeic acid, arteannunin b, deoxyartemisinin, quercetin, scopolin, sitogluside, scopoletin, scoparone, apigenin, artemether, artemetin, Artemisnic acid, artemetil, artesunate, casticin, chrysoplenetin. Among all these APIGENIN and CHRYSOPLENETIN are selected as

the top two compounds but out of them **CHRYSOPLENETIN** is selected as the lead compound, as much work is already done on apigenin.

4.8 Drug Identification against Covid-19

With the emergence of the disease, many FDA-approved drugs were utilized for drug repurposing finding the best treatment against the virus. One of the drugs that have been in use in different countries like the UK, Brazil, India, Pakistan, and many more is Azithromycin. Though the use of this medicine has increased during this whole pandemic this drug is still in clinical trials for action against corona virus [69, 70].

4.8.1 Azithromycin

Azithromycin is an antibiotic that is used against mycobacterium. It is an FDA-approved drug that can be used for the treatment of infections occurred in the lungs, skin, sinuses, and other body parts. With that azithromycin may prove beneficial against malaria when this drug is taken with a combination of certain other drugs [69]. Though it is an antibiotic that acts against gram-positive bacteria azithromycin has proven to show positive in vitro results against viruses like Ebola, influenza, flavivirus, HIV, and corona (MERS and SARS) [26, 27].

4.8.2 Azithromycin Docking

Table 4.11 shows the docking result of Azithromycin. The table indicates that azithromycin has a binding score of -6.8.

The docking results of Azithromycin with M^{pro} shows that it has quite a good binding score. And has five hydrogen bond donars, and fourteen hydrogen bond acceptors that breaks one of the Lipinski rule. Azithromycin has seven numbers of rotatable bonds.

TABLE 4.11: Docking results of Azithromycin

Compound	Binding Score	Cavity size	HBD	HBA	logP	Mol. Weight g/ mol	Rotatable Bonds	Grid Map
Azithromycin	-6.8	258	5	14	1.9007	748.996	7	71.716

4.9 Azithromycin Comparison with Lead Compound

The standard drug azithromycin is compared with the lead compound chrysoplenetin and their physicochemical and pharmacokinetic properties are compared for the assessment of bioavailability, efficiency, safety, and drug-likeness.

The table 4.12 shows that Azithromycin breaks two of Lipinski's rules that are of molecular weight and H-bond acceptor as the molecular weight of azithromycin is 748.996 which is more than 500 according to Lipinski and that for H-bond acceptor azithromycin accepts 14 hydrogens.

But according to Lipinski it should not be more than 10, whereas Chrysoplenetin follows all rules of LogP, Molecular weight, H-bond acceptor and H-bond donar according to Lipinski.

TABLE 4.12: Lipinski Rule Comparison

S. No.	Name of Compound	Log P-value	Molecular Weight g/mol	H-bond acceptor	H-bond donor
1.	Azithromycin	1.9007	748.996	14	05
2.	Chrysoplenetin	2.9056	374.3	8	2

4.10 ADMET Properties Comparison

The ADMET properties comparison is done to check the absorption, distribution, metabolic excretion, and toxicity properties of the drug and the lead compound for finding a better drug candidate [71-73].

4.10.1 Toxicity Comparison

The toxicity of both the standard drug and lead compound is based upon 9 models. Model 1 of AMES toxicity shows that both the standard and lead compounds are not mutagenic. Model 2 of Maximum tolerated dose gives that if the value is equal or less to 0.477 log mg/kg/day then it is considered low and greater values are considered high. The table below shows that chrysopenetin has a low value of tolerated dose. 3rd model is of hERG I and II inhibitors both these compounds are not inhibitors. 4th model of oral rat acute toxicity is used to assess the relative toxicity. Model 5 of oral rat chronic toxicity gives the values of the lowest dose that could result in an adverse effect. Model 6 of hepatotoxicity shows either the drug can cause damage to the liver. The table shows that azithromycin is hepatotoxic. For the dermal products model, 7 is used for checking the sensitivity towards the skin. Both the standard and lead compounds are not sensitive to skin. Model 8 uses *T. pyriformis* and model 9 uses minnows to check the toxicity. For *T. pyriformis* value > -0.5 is considered toxic according to which azithromycin is somewhat toxic and for minnow toxicity values below 0.5mM are considered toxic and both compounds pass this toxicity test. Table 4.13 shows the comparative values of toxicity of azithromycin and chrysopenetin.

TABLE 4.13: Toxicity Properties Comparison

S.No.	Model Name	Azithromycin	Chrysopenetin
1.	AMES Toxicity	No	No
2.	Max. tolerated dose (human)	1.927	0.491
3.	hERG I inhibitor	No	No
4.	hERG II inhibitor	No	No

5.	Oral rat acute toxicity	2.769	2.324
6.	Oral rat chronic toxicity	1.991	1.773
7.	Hepatotoxicity	Yes	No
8.	Skin sensitization	No	No
9.	t.pyriformis toxicity	0.285	0.313
10.	Minnow toxicity	7.8	2.248

4.10.2 Absorption Properties Comparison

The parameter of absorption is based upon 6 models. The water solubility model gives the value of solubility of the compound in water when at 25°C. The model of CaCO₂ solubility is used to predict the drug absorption when given orally. Values greater than 0.90 are considered to have high intestinal absorption, which means chrysoplenetin is absorbed more than azithromycin. Value of intestinal absorption model less than 30% is considered to be poorly absorbed. The given values of both the standard and lead compound show that chrysoplenetin has high intestinal absorption. For the transdermal drugs the skin permeability model, value less than $\log K_p > -2.5$ is considered low, according to this both the compounds pass the skin permeability test. The P-glycoprotein substrate model is very important as P-glycoprotein is an ABC transporter and acts as a biological barrier. Both chrysoplenetin and azithromycin act as the substrates. The last model of P-glycoprotein inhibitors shows that whether the compound is an inhibitor or not. The table 4.14 shows that Chrysoplenetin is an inhibitor of P-glycoprotein II whereas azithromycin is the inhibitor of P-glycoprotein I.

TABLE 4.14: Absorption Properties Comparison

S. No.	Reference drug	Azithromycin	Chrysoplenetin
1.	Water Solubility	-4.133	-3.605
2.	CaCO ₂ Solubility	-0.211	1.393
3.	Intestinal Absorption (human)	45.808	99.856
4.	Skin Permeability	-2.742	-2.743

5.	P-glycoprotein substrate	Yes	Yes
6.	P-glycoprotein I inhibitor	Yes	No
7.	P-glycoprotein II inhibitor	No	Yes

4.10.3 Metabolic Properties Comparison

Cytochrome P450 is found in the liver mainly and is held responsible for oxidizing the xenobiotic so that they can be excreted easily out from the body hence making cytochrome P450 a detoxification enzyme. Some drugs are activated by it or some are deactivated. So it is important to assess that whether a compound is a P450 substrate or not, and whether it is an inhibitor to P450 or not. The table 4.15 shows that azithromycin is a CYP3A4 substrate and Chrysoplenetin is a CYP3A4 substrate and CYP1A2 inhibitor, CYP2C19 inhibitor, and CYP3A4 inhibitor.

TABLE 4.15: Metabolic Properties Comparison

S. No.	Reference Drug	Azithromycin	Chrysoplenetin
1.	CYP2D6 substrate	No	No
2.	CYP3A4 substrate	Yes	Yes
3.	CYP1A2 inhibitor	No	Yes
4.	CYP2C19 inhibitor	No	Yes
5.	CYP2C9 inhibitor	No	No
6.	CYP2D6 inhibitor	No	No
7.	CYP3A4 inhibitor	No	Yes

4.10.4 Distribution Properties Comparison

Table 4.16 shows the comparative distribution properties of Azithromycin and Chrysoplenetin. The distribution parameter is based upon 4 models. The volume of distribution (VD_{ss}) is the uniform distribution of the drug in the blood plasma and if this value is above 2.81 L/kg then the drug is distributed more in the tissues

rather than in the blood plasma. Both azithromycin and chrysopenetin have a reasonable VDss value. 2nd model is based upon the fraction unbound of the drugs in the plasma as bounded drugs affect the efficiency of the drugs. The given value is the amount of the drug which remains unbounded.

For BBB permeability if the value is greater than 0.3 logBB then that drug can easily cross the blood-brain barriers and if the value is less than -1 logBB then the drug is not or poorly distributed to the brain. From these values, it is clear that Azithromycin has a low value hence it would be poorly distributed to the brain.

Similarly, the model for CNS is based on the values that if the logPS > -2 then that drug can easily penetrate to the CNS while those having value of logPS < -3 will be unable to penetrate the central nervous system. Azithromycin has a low value hence it will not be able to pass the central nervous system.

TABLE 4.16: Distribution Properties Comparison

S. No.	Reference Drug	Azithromycin	Chrysopenetin
1.	VDss (human)	-0.214	-0.161
2.	Fraction unbound (human)	0.512	0.103
3.	BBB Permeability	-1.857	-1.043
4.	CNS Permeability	-3.777	-3.226

4.10.5 Excretion Properties Comparison

The value of total clearance is a combination of hepatic and renal clearance and is important so that the dose rates of the drugs can be assessed. chrysopenetin has more total clearance than azithromycin. The 2nd model is of the Renal OCT2 (organic cation transporter 2) and this transporter helps in the renal clearance of drugs and other compounds. Being an OCT2 substrate can have an adverse effect in correlation with inhibitors. So both azithromycin and chrysopenetin are not Renal OCT2 substrates. Table 4.17 shows the values of excretory properties of azithromycin and chrysopenetin.

TABLE 4.17: Excretion Properties Comparison

S. No.	Reference Drug	Azithromycin	Chrysoplenetin
1.	Total Clearance	-0.424	0.627
2.	Renal OCT2 Substrate	No	No

4.11 Physiochemical Properties Comparison

For determining the fundamental properties of the compounds physiochemical properties are studied. Through this screening, it shows that azithromycin has 38 carbon atoms, 72 hydrogen atoms, 2 nitrogen atoms, and 12 oxygen atoms whereas chrysoplenetin has 19 carbon atoms, 18 hydrogen atoms, and 8 oxygen atoms. This shows that chrysoplenetin is a simple bio-compound in relevance to azithromycin. Azithromycin can donate 5 hydrogen atoms whereas chrysoplenetin can donate only 2 hydrogen atoms showing the oxidation state. Azithromycin can accept 14 Hydrogen atoms which do not fall under the Lipinski rule.

Although the Log P value of azithromycin is less than chrysoplenetin the molecular weight of azithromycin is far greater than chrysoplenetin and also it does not fall under the Lipinski rule. In a comparison of rotatable bonds azithromycin has 7 whereas chrysoplenetin has only five rotatable bonds. Table 4.18 shows the comparison of physiochemical properties of azithromycin and chrysoplenetin.

TABLE 4.18: Physiochemical Properties Comparison

S. No.	Drug	Mol. Formula	H-bond donor	H-bond acceptor	Log P-value	Mol. Weight g/mol	Rotatable Bonds
1.	Azithromycin	C ₃₈ H ₇₂ - N ₂ O ₁₂	5	14	1.9007	748.996	7
2.	Chrysoplenetin	C ₁₉ H ₁₈ - O ₈	2	8	2.9056	374.3	5

4.12 Docking Score Comparison

Both the standard and the lead compound were docked against the M^{pro} and the docking result gives us the best binding score. Table 4.19 shows that the lead compound which is chrysopenetin has a much higher vina score than that of the standard drug which is azithromycin. The binding score of azithromycin is -6.8 and that for chrysopenetin is -7.7 which is higher than that of the standard drug. This result shows that chrysopenetin can block the M^{pro} or bind with it more efficiently than that of azithromycin.

TABLE 4.19: Docking Score Comparison

S.No.	Compound	Binding Score
1.	Azithromycin	-6.8
2.	Chrysopenetin	-7.7

4.13 Docking Analysis Comparison

The docking results are analyzed by LigPlot based on the number of hydrogen bonds, number of hydrophobic interactions, number of interacting amino acids, and that of steric interactions. Figure 4.32 and 4.33 shows the docking results of azithromycin and chrysopenetin. Figure 4.32 shows that azithromycin has formed only one hydrogen bond and ten hydrophobic interactions

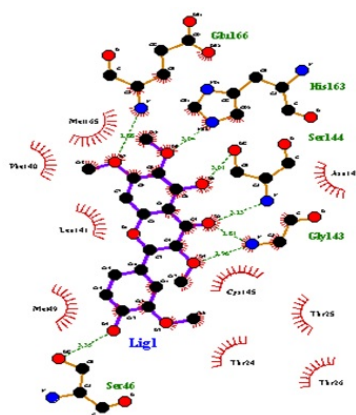


FIGURE 4.31: Interaction of azithromycin with the receptor

Figure 4.33 shows that chrysoplenetin has formed seven hydrogen bonds and nine hydrophobic interactions.

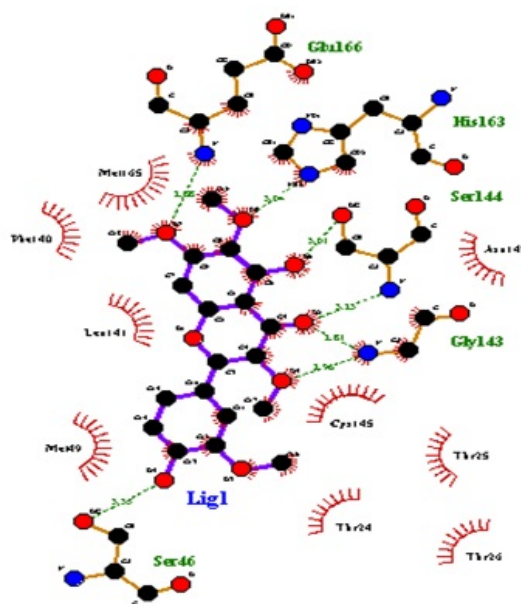


FIGURE 4.32: Interaction of chrysoplenetin with receptor

The details of hydrogen and hydrophobic interactions are mentioned in the Table 4.20. chrysoplenetin forms seven hydrogen bonds whereas azithromycin form only 1 hydrogen bond, this is mainly because chrysoplenetin O2, O4, O5, O6, O7, and O8 has made interactions with the receptor. Azithromycin makes 10 hydrophobic interactions whereas chrysoplenetin makes 9 of them. With all this information chrysoplenetin succeeds to be much better than azithromycin.

The table 4.20 shows that Cys145, Gly143, Ser144, Leu141, Phe140, Asn142, Glu166, Met165, His164, Gln189 participates in forming hydrophobic interaction between the protein and azithromycin. The oxygen atom of Thr 190 forms a hydrogen bond with the third oxygen of azithromycin forming a O-Thr190-O3 bond.

Whereas Asn142, Cys145, Thr25, Thr24, Thr26, Met49, Leu141, Phe140, Met165 participates in forming hydrophobic interaction between the protein and chrysoplenetin. The oxygen atom of Ser 46 termed as OG forms a hydrogen atom with O4 of chrysoplenetin forming a OG-Ser46-O4 bond. The nitrogen of Gly143 bonds to 5th oxygen of chrysoplenetin, similarly the nitrogen of Gly143 and Ser 144 forms

a bond with second oxygen of chrysopenetin. These three bonds are represented as N-Gly143-O5, N-Gly143-O2, N-Ser144-O2 respectively. The oxygen of Ser 144 forms a bond with the sixth oxygen of chrysopenetin OG-Ser144-O6. With that the nitrogen of His163 forms bond with the oxygen at eighth position of chrysopenetin NE2-His163-O8. The nitrogen of Glu166 forms a bond with oxygen at seventh number of chrysopenetin represented as N-Glu166-O7.

TABLE 4.20: Docking Analysis Comparison

S. No.	Ligand Name	Binding Energy	No. of HBs	Hydrogen Bonding		Hydrophobic Bonding
				Amino Acids	Distance	
1.	Azithromycin	-6.8	1	O-Thr190-O3	2.90	Cys145
						Gly143
						Ser144
						Leu141
						Phe140
						Asn142
						Glu166
						Met165
						His164
						Gln189
2.	Chrysopenetin	-7.7	7	OG-Ser46-O4	3.35	Asn142
						Cys145
						Thr25
						Thr24
						Thr26
						Met49
						Leu141
						Phe140
Met165						

Chapter 5

Conclusion and Future Prospects

Covid-19 has created a havoc for human race structural analysis revealed its non-structural protein M^{pro} to be an active drug target, for this purpose many drugs were repurposed out of these azithromycin was commonly used in different countries. Many other natural compounds were identified against the target. Some plants were investigated for their efficiency against M^{pro} . One of the plant under observation was *Artemisia annua*. This study aimed to screen out the active constituents in the plant *Artemisia annua*. In silico molecular docking served the purpose for this screening of the inhibitory compounds against M^{pro} that could be helpful in drug development to combat the challenge of Covid-19. From plant *Artemisia annua* 25 ligands showing antiviral properties were selected to be docked against the main protease of coronavirus.

The structure of all the 25 ligands were downloaded from PubChem and then their energies were minimized by Chem3D ultra. The protein structure was downloaded from PDB. All the ligands were docked against the receptor protein via CB Dock. The results were visualized using PyMol and were analyzed through LigPlot. Next the ligands were screened out on the basis of Lipinski rule of five and drug ADMET properties. Out of those 25 ligands, rutin was first screened out based on Lipinski's rule, and based on second screening artemisinin, dihydroartemisinin, and beta-sitosterol were knocked out. After these 21 ligands were left and out of those chrysoplenetin and apigenin were the two best active ligands.

Based on the inhibition effect due to hydrophobic and hydrogen bonding chryso-
plenetin was selected as a lead against the standard drug azithromycin. With the
final results, it was cleared that chrysoplenetin can bind far better to M^{pro} than
that of azithromycin and can be a better drug candidate.

5.1 Recommendations

As per the findings of this research *Artemisia annua* active constituent like api-
genin, quercetin, artemetin, scopolin, artesunate, deoxyartemesnin, casticin and
sitogluside have also shown a positive result in response to M^{pro} so these lig-
ands should be studied and exploited more for their effect against SARS-CoV2.
Previously *Artemisia annua* has been used as anti-viral, anti-inflammatory, anti-
oxidants, and anti-malarial for this reason *Artemisia annua* should be explored
more for its effectiveness against covid-19

Bibliography

1. Wang, C., Horby, P. W., Hayden, F. G., & Gao, G. F. (2020). A novel coronavirus outbreak of global health concern. *The lancet*, 395(10223), 470-473.
2. Machhi, J., Herskovitz, J., Senan, A. M., Dutta, D., Nath, B., Oleynikov, M. D., ... & Kevadiya, B. D. (2020). The natural history, pathobiology, and clinical manifestations of SARS-CoV-2 infections. *Journal of Neuroimmune Pharmacology*, 1-28.
3. Shereen, M. A., Khan, S., Kazmi, A., Bashir, N., & Siddique, R. (2020). COVID-19 infection: Origin, transmission, and characteristics of human coronaviruses. *Journal of advanced research*, 24, 91-98.
4. Huang, C., Wang, Y., Li, X., Ren, L., Zhao, J., Hu, Y., ... & Cao, B. (2020). Clinical features of patients infected with 2019 novel coronavirus in Wuhan, China. *The lancet*, 395(10223), 497-506.
5. Ziebuhr, J., Snijder, E. J., & Gorbalenya, A. E. (2000). Virus-encoded proteinases and proteolytic processing in the Nidovirales. *Microbiology*, 81(4), 853-879.
6. Snijder, E. J., Bredenbeek, P. J., Dobbe, J. C., Thiel, V., Ziebuhr, J., Poon, L. L., ... & Gorbalenya, A. E. (2003). Unique and conserved features of genome and proteome of SARS-coronavirus, an early split-off from the coronavirus group 2 lineage. *Journal of molecular biology*, 331(5), 991-1004.

7. Le, T. T., Andreadakis, Z., Kumar, A., Román, R. G., Tollefsen, S., Saville, M., & Mayhew, S. (2020). The COVID-19 vaccine development landscape. *Nat Rev Drug Discov*, 19(5), 305-306.
8. Hunziker, P. (2021). Vaccination strategies for minimizing loss of life in Covid-19 in a Europe lacking vaccines. Available at SSRN 3780050.
9. Boni, M. F., Lemey, P., Jiang, X., Lam, T. T. Y., Perry, B. W., Castoe, T. A., ... & Robertson, D. L. (2020). Evolutionary origins of the SARS-CoV-2 sarbecovirus lineage responsible for the COVID-19 pandemic. *Nature Microbiology*, 5(11), 1408-1417.
10. Chen, Y., Liu, Q., & Guo, D. (2020). Emerging coronaviruses: genome structure, replication, and pathogenesis. *Journal of medical virology*, 92(4), 418-423.
11. Law, S., Leung, A. W., & Xu, C. (2020). Is the traditional Chinese herb “*Artemisia annua*” possible to fight against COVID-19?. *Integrative Medicine Research*, 9(3).
12. Haq, F. U., Roman, M., Ahmad, K., Rahman, S. U., Shah, S. M. A., Suleman, N., ... & Ullah, W. (2020). *Artemisia annua*: trials are needed for COVID-19. *Phytotherapy Research*.
13. Zhu, N., Zhang, D., Wang, W., Li, X., Yang, B., Song, J., ... & Tan, W. (2020). A novel coronavirus from patients with pneumonia in China, 2019. *New England journal of medicine*, 382:727-733.
14. Diseases, T. L. I. (2020). Challenges of coronavirus disease 2019. *The Lancet. Infectious Diseases*, 20(3), 261.
15. ul Qamar, M. T., Alqahtani, S. M., Alamri, M. A., & Chen, L. L. (2020). Structural basis of SARS-CoV-2 3CLpro and anti-COVID-19 drug discovery from medicinal plants. *Journal of pharmaceutical analysis*, 10(4), 313-319.
16. Xu, X., Chen, P., Wang, J., Feng, J., Zhou, H., Li, X., ... & Hao, P. (2020). Evolution of the novel coronavirus from the ongoing Wuhan outbreak and

- modeling of its spike protein for risk of human transmission. *Science China Life Sciences*, 63(3), 457-460.
17. Anand, K., Ziebuhr, J., Wadhwani, P., Mesters, J. R., & Hilgenfeld, R. (2003). Coronavirus main proteinase (3CLpro) structure: basis for design of anti-SARS drugs. *Science*, 300(5626), 1763-1767.
 18. Hoffmann, M., Kleine-Weber, H., Schroeder, S., Krüger, N., Herrler, T., Erichsen, S., ... & Pöhlmann, S. (2020). SARS-CoV-2 cell entry depends on ACE2 and TMPRSS2 and is blocked by a clinically proven protease inhibitor. *cell*, 181(2), 271-280.
 19. Ghosh, S., Dellibovi-Ragheb, T. A., Kerviel, A., Pak, E., Qiu, Q., Fisher, M., ... & Altan-Bonnet, N. (2020). β -Coronaviruses use lysosomes for egress instead of the biosynthetic secretory pathway. *Cell*, 183(6), 1520-1535.
 20. Docea, A. O., Tsatsakis, A., Albulescu, D., Cristea, O., Zlatian, O., Vinceti, M., ... & Calina, D. (2020). A new threat from an old enemy: Re-emergence of coronavirus. *International Journal of molecular medicine*, 45(6), 1631-1643.
 21. Drosten, C., Günther, S., Preiser, W., Van Der Werf, S., Brodt, H. R., Becker, S., ... & Doerr, H. W. (2003). Identification of a novel coronavirus in patients with the severe acute respiratory syndrome. *New England journal of medicine*, 348(20), 1967-1976.
 22. Boni, M. F., Lemey, P., Jiang, X., Lam, T. T. Y., Perry, B. W., Castoe, T. A., ... & Robertson, D. L. (2020). Evolutionary origins of the SARS-CoV-2 sarbecovirus lineage responsible for the COVID-19 pandemic. *Nature Microbiology*, 5(11), 1408-1417.
 23. Danielle Dresden [January 11, 2021] Coronavirus(Covid-19) vaccine-what to know. <https://www.medicalnewstoday.com/articles/coronavirus-vaccine>.
 24. Farag, A., Wang, P., Ahmed, M., & Sadek, H. (2020). Identification of FDA approved drugs targeting COVID-19 virus by structure-based drug repositioning.

25. Mostafa, A., Kandeil, A., AMM Elshaier, Y., Kutkat, O., Moatasim, Y., Rashad, A. A., ... & Ali, M. A. (2020). FDA-approved drugs with potent in vitro antiviral activity against severe acute respiratory syndrome coronavirus 2. *Pharmaceuticals*, 13(12), 443.
26. Drożdżal, S., Rosik, J., Lechowicz, K., Machaj, F., Kotfis, K., Ghavami, S., & Łos, M. J. (2020). FDA approved drugs with pharmacotherapeutic potential for SARS-CoV-2 (COVID-19) therapy. *Drug resistance updates*, 100719.
27. Gautret, P., Lagier, J. C., Parola, P., Meddeb, L., Mailhe, M., Doudier, B., ... & Raoult, D. (2020). Hydroxychloroquine and azithromycin as a treatment of COVID-19: results of an open-label non-randomized clinical trial. *International journal of antimicrobial agents*, 56(1), 105949.
28. Schögler, A., Kopf, B. S., Edwards, M. R., Johnston, S. L., Casaulta, C., Kieninger, E., ... & Alves, M. P. (2015). Novel antiviral properties of azithromycin in cystic fibrosis airway epithelial cells. *European respiratory journal*, 45(2), 428-439.
29. Menzel, M., Akbarshahi, H., Bjermer, L., & Uller, L. (2016). Azithromycin induces anti-viral effects in cultured bronchial epithelial cells from COPD patients. *Scientific reports*, 6(1), 1-11.
30. Cai, M., Bonella, F., Dai, H., Sarria, R., Guzman, J., & Costabel, U. (2013). Macrolides inhibit cytokine production by alveolar macrophages in bronchiolitis obliterans organizing pneumonia. *Immunobiology*, 218(6), 930-937.
31. Benarba, B., & Pandiella, A. (2020). Medicinal plants as sources of active molecules against COVID-19. *Frontiers in Pharmacology*, 11.
32. Hong-Zhi, D. U., Xiao-Ying, H. O. U., Yu-Huan, M. I. A. O., Huang, B. S., & Da-Hui, L. I. U. (2020). Traditional Chinese Medicine: an effective treatment for 2019 novel coronavirus pneumonia (NCP). *Chinese journal of natural medicines*, 18(3), 206-210.

33. El Alami, A., Fattah, A., & Chait, A. (2020). Medicinal plants used for the prevention purposes during the covid-19 pandemic in Morocco. *Journal of analytical sciences and applied biotechnology*, 2(1), 2-1.
34. Patten, G. S., Abeywardena, M. Y., & Bennett, L. E. (2016). Inhibition of angiotensin-converting enzyme, angiotensin II receptor blocking, and blood pressure-lowering bioactivity across plant families. *Critical Reviews in Food Science and Nutrition*, 56(2), 181-214.
35. Valles, J., Garcia, S., Hidalgo, O., Martin, J., Pellicer, J., Sanz, M., & Garnatje, T. (2011). Biology, genome evolution, biotechnological issues, and research including applied perspectives in *Artemisia* (Asteraceae). *Advances in botanical research*, 60, 349-419.
36. Willcox, M. (2009). *Artemisia* species: from traditional medicines to modern antimalarials—and back again. *The Journal of Alternative and Complementary Medicine*, 15(2), 101-109.
37. Čavar, S., Maksimović, M., Vidic, D., & Parić, A. (2012). Chemical composition and antioxidant and antimicrobial activity of essential oil of *Artemisia annua* L. from Bosnia. *Industrial Crops and Products*, 37(1), 479-485.
38. Li, K. M., Dong, X., Ma, Y. N., Wu, Z. H., Yan, Y. M., & Cheng, Y. X. (2019). Antifungal coumarins and lignans from *Artemisia annua*. *Fitoterapia*, 134, 323-328.
39. Septembre-Malaterre, A., Lalarizo Rakoto, M., Marodon, C., Bedoui, Y., Nakab, J., Simon, E., ... & Gasque, P. (2020). *Artemisia annua*, a Traditional Plant Brought to Light. *International Journal of Molecular Sciences*, 21(14), 4986.
40. Morris, G. M., & Lim-Wilby, M. (2008). Molecular docking. In *Molecular modeling of proteins* (pp. 365-382). Humana Press.

41. Yuriev, E., & Ramsland, P. A. (2013). Latest developments in molecular docking: 2010–2011 in review. *Journal of Molecular Recognition*, 26(5), 215-239.
42. Zhang, L., Lin, D., Sun, X., Curth, U., Drosten, C., Sauerhering, L., ... & Hilgenfeld, R. (2020). Crystal structure of SARS-CoV-2 main protease provides a basis for the design of improved α -ketoamide inhibitors. *Science*, 368(6489), 409-412.
43. Kumar, V., Tan, K. P., Wang, Y. M., Lin, S. W., & Liang, P. H. (2016). Identification, synthesis and evaluation of SARS-CoV and MERS-CoV 3C-like protease inhibitors. *Bioorganic & medicinal chemistry*, 24(13), 3035-3042.
44. Zhou, J., Xie, G., & Yan, X. (2011). Encyclopedia of traditional Chinese medicines. *Isolat Compound AB*, 1, 455.
45. He, J., Hu, L., Huang, X., Wang, C., Zhang, Z., Wang, Y., ... & Ye, W. (2020). Potential of coronavirus 3C-like protease inhibitors for the development of new anti-SARS-CoV-2 drugs: Insights from structures of protease and inhibitors. *International journal of antimicrobial agents*, 56(2), 106055.
46. Wu, C., Liu, Y., Yang, Y., Zhang, P., Zhong, W., Wang, Y., ... & Li, H. (2020). Analysis of therapeutic targets for SARS-CoV-2 and discovery of potential drugs by computational methods. *Acta Pharmaceutica Sinica B*, 10(5), 766-788.
47. Tsai, K. C., Chen, S. Y., Liang, P. H., Lu, I. L., Mahindroo, N., Hsieh, H. P., ... & Wu, S. Y. (2006). Discovery of a novel family of SARS-CoV protease inhibitors by virtual screening and 3D-QSAR studies. *Journal of medicinal chemistry*, 49(12), 3485-3495.
48. Garg, V. K., Avashthi, H., Tiwari, A., Jain, P. A., Ramkete, P. W., Kayastha, A. M., & Singh, V. K. (2016). MFPPi–multi FASTA ProtParam interface. *Bioinformatics*, 12(2), 74.

49. DeLano, W. L. (2002). Pymol: An open-source molecular graphics tool. *CCP4 Newsletter on protein crystallography*, 40(1), 82-92.
50. Hunter, S., Jones, P., Mitchell, A., Apweiler, R., Attwood, T. K., Bateman, A., ... & Yong, S. Y. (2012). InterPro in 2011: new developments in the family and domain prediction database. *Nucleic acids research*, 40(D1), D306-D312.
51. Bolton, E. E., Wang, Y., Thiessen, P. A., & Bryant, S. H. (2008). PubChem: integrated platform of small molecules and biological activities. In *Annual reports in computational chemistry*, Elsevier, 4, 217-241.
52. Pagadala, N. S., Syed, K., & Tuszynski, J. (2017). Software for molecular docking: a review. *Biophysical reviews*, 9(2), 91-102.
53. Yuriev, E., Holien, J., & Ramsland, P. A. (2015). Improvements, trends, and new ideas in molecular docking: 2012–2013 in review. *Journal of Molecular Recognition*, 28(10), 581-604.
54. Yuan, S., Chan, H. S., & Hu, Z. (2017). Using PyMOL as a platform for computational drug design. *Wiley Interdisciplinary Reviews: Computational Molecular Science*, 7(2), e1298.
55. Mostafa, S. I. (2007). Mixed ligand complexes with 2-piperidine-carboxylic acid as primary ligand and ethylene diamine, 2, 2'-bipyridyl, 1, 10-phenanthroline and 2 (2'-pyridyl) quinoxaline as secondary ligands: preparation, characterization and biological activity. *Transition Metal Chemistry*, 32(6), 769-775.
56. Ntie-Kang, F. (2013). An in silico evaluation of the ADMET profile of the StreptomeDB database. *Springerplus*, 2(1), 1-11.
57. Lipinski, C. A. (2004). Lead-and drug-like compounds: the rule-of-five revolution. *Drug Discovery Today: Technologies*, 1(4), 337-341.
58. Farabi, S., Saha, N. R., Khan, N. A., & Hasanuzzaman, M. (2020). Prediction of SARS-CoV-2 Main Protease Inhibitors from Several Medicinal Plant Compounds by Drug Repurposing and Molecular Docking Approach. *ChemRxiv*. 12440024.v1

59. Russell, B., Moss, C., George, G., Santaolalla, A., Cope, A., Papa, S., & Van Hemelrijck, M. (2020). Associations between immune-suppressive and stimulating drugs and novel COVID-19—a systematic review of current evidence. *ecancermedicalsecience*, 14.
60. Wang, K. Y., Liu, F., Jiang, R., Yang, X., You, T., Liu, X., ... & Yang, H. (2020). Structure of Mpro from COVID-19 virus and discovery of its inhibitors. *Nature*.
61. Garg, V. K., Avashthi, H., Tiwari, A., Jain, P. A., Ramkete, P. W., Kayastha, A. M., & Singh, V. K. (2016). MFPPi—multi FASTA ProtParam interface. *Bioinformatics*, 12(2), 74.
62. Morya, V. K., Yadav, S., Kim, E. K., & Yadav, D. (2012). In silico characterization of alkaline proteases from different species of *Aspergillus*. *Applied biochemistry and biotechnology*, 166(1), 243-257.
63. Bhattacharya, P., & Patel, T. N. (2021). Deregulation of MMR-Related Pathways and Anticancer Potential of Curcuma Derivatives—A Computational Approach.
64. İstifli, E. S., Şihoğlu Tepe, A., Sarikürkcü, C., & Tepe, B. (2020). Interaction of certain monoterpene hydrocarbons with the receptor binding domain of 2019 novel coronavirus (2019-nCoV), transmembrane serine protease 2 (TM-PRSS2), cathepsin B, and cathepsin L (CatB/L) and their pharmacokinetic properties. *Turkish journal of biology = Turk biyoloji dergisi*, 44(3), 242–264.
65. Khurshid, Z. (2021). Determination of Potential Antioxidants of *Artemisia annua* by Computational Approaches (Doctoral dissertation, Capital University).
66. Yabrir, B., Belhassan, A., Lakhli, T., Salgado M, G., Bouachrine, M., Munoz C, P., ... & Ramirez T, R. (2021). Minor composition compounds of Algerian herbal medicines as inhibitors of SARS-CoV-2 main protease: Molecular Docking and ADMET properties prediction. *Journal of the Chilean Chemical Society*, 66(1), 5067-5074.

67. Taofeek, O. (2020). Molecular Docking and Admet Analyses of Photochemicals from *Nigella sativa* (blackseed), *Trigonella foenum-graecum* (Fenu-greek) and *Anona muricata* (Soursop) on SARS-CoV-2 Target. *ScienceOpen Preprints*.
68. Sankar, M., Ramachandran, B., Pandi, B., Mutharasappan, N., Ramasamy, V., Prabu, P. G., Shanmugaraj, G., Wang, Y., Muniyandai, B., Rathinasamy, S., Chandrasekaran, B., Bayan, M. F., Jeyaraman, J., Halliah, G. P., & Ebenezer, S. K. (2021). In silico Screening of Natural Phytocompounds Towards Identification of Potential Lead Compounds to Treat COVID-19. *Frontiers in molecular biosciences*, 8, 637122.
69. Oliver, M. E., & Hinks, T. S. (2020). Azithromycin in viral infections. *Reviews in medical virology*, e2163.
70. Abaleke, E., Abbas, M., Abbasi, S., Abbott, A., Abdelaziz, A., Abdelbadiee, S., ... & Allison, K. (2021). Azithromycin in patients admitted to hospital with COVID-19 (RECOVERY): a randomised, controlled, open-label, platform trial. *The Lancet*, 397(10274), 605-612.
71. Kakad Smita, P., Kshirsagar Sanajy, J., Asole Rahul, K., Pathade Nikhil, V., & Vyavahare Maheshwari, D. (2020). Review on Current Drug Therapy and Use of Natural Products in the Management of COVID 19. *Journal of Seybold Report ISSN NO*, 1533, 9211.
72. Parnham, M. J., Haber, V. E., Giamarellos-Bourboulis, E. J., Perletti, G., Verleden, G. M., & Vos, R. (2014). Azithromycin: mechanisms of action and their relevance for clinical applications. *Pharmacology & therapeutics*, 143(2), 225-245.
73. Daina, A., Michielin, O., & Zoete, V. (2017). SwissADME: a free web tool to evaluate pharmacokinetics, drug-likeness and medicinal chemistry friendliness of small molecules. *Scientific reports*, 7(1), 1-13.